I&EC research
Industrial & Engineering Chemistry Research

Article

pubs.acs.org/IECR

Theoretical Study of Intermolecular Chain Transfer to Polymer Reactions of Alkyl Acrylates

Nazanin Moghadam,[†] Shi Liu,[‡] Sriraj Srinivasan,[§] Michael C. Grady,[#] Andrew M. Rappe,[‡] and Masoud Soroush*,[†]

[†]Department of Chemical and Biological Engineering, Drexel University, Philadelphia, Pennsylvania 19104, United States

[‡]The Makineni Theoretical Laboratories, Department of Chemistry, University of Pennsylvania, Philadelphia, Pennsylvania 19104-6323, United States

[§]Arkema Inc., 900 First Avenue, King of Prussia, Pennsylvania 19406, United States

[#]DuPont Experimental Station, Wilmington, Delaware 19898, United States

Supporting Information

ABSTRACT: Mechanisms of intermolecular chain transfer to polymer (CTP) reactions in monomer self-initiated polymerization of alkyl acrylates, such as methyl acrylate, ethyl acrylate, and *n*-butyl acrylate, are studied using density functional theory calculations. Dead polymer chains with three different structures are considered, and three types of hybrid density functionals and four basis sets are used. The energy barrier and rate constant of each reaction are calculated using the transition state theory and the rigid rotor harmonic oscillator approximation. The study indicates that tertiary hydrogens of dead polymers formed by disproportionation reactions are most likely to be transferred to live polymer chains in CTP reactions. The length of the polymer chain has little effect on the calculated activation energies and transition-state geometries in all CTP mechanisms explored in this study. Moreover, CTP reactions of methyl, ethyl, and butyl acrylates have similar energy barriers and rate constants. The application of the integral equation formalism-polarizable continuum model results in higher CTP energy barriers. This increase in the predicted CTP energy barriers is larger in *n*-butanol than in *p*-xylene. However, the application of the conductor-like screening model does not affect the predicted CTP kinetic parameters.

1. INTRODUCTION

Acrylic binder resins are used in paint and coating formulations.[1] Environmental regulations, which require the volatile organic content of resins to be less than 300 ppm, have caused changes in the basic design of resins used in automobile coating formulations.[2] High temperature (>100 °C) free-radical polymerization allows production of low-molecular-weight high-polymer-content acrylic resins that have low viscosity.[3−5] However, in high temperature polymerization, secondary reactions[6] such as β-scission,[7] monomer self-initiation,[8−10] and intra- and intermolecular chain transfer to polymer (CTP) reactions[11,12] strongly affect properties of the polymer products.[6,7,13−18]

There are two types of CTP reactions: intramolecular and intermolecular. In an intramolecular chain transfer (backbiting) reaction, a secondary radical (live chain) abstracts a hydrogen atom from its backbone, producing a midchain radical.[11,19−21] In an intermolecular chain transfer reaction, however, a live polymer chain abstracts a hydrogen atom from a dead polymer.[15,19] Prior to this work, it was inconclusive which dead polymer structure was most likely to provide the hydrogen atom during CTP reactions. Although at low polymer concentrations intramolecular CTP is dominant,[19] at high polymer concentrations intermolecular CTP is dominant.[15,19,22−26] The new radicals generated by CTP reactions propagate to form branches or terminate by coupling with other propagating radicals.[15] The kinetic parameters of backbiting reactions of chain-end and midchain radicals were investigated by applying the density functional theory (DFT) approach.[20] It was found experimentally that hydrogen bonding has a disruptive effect on acrylate backbiting mechanisms, and the level of branching can be reduced by choosing an appropriate solvent.[27] The contribution of CTP to the level of branching was explored for controlled radical polymerization (CRP)[28] and conventional free radical polymerization (FRP) of butyl acrylate (BA), and the level of branches as a function of transient lifetime was reported.[23,26] The role of midchain radicals, formed through inter- and intramolecular CTP reactions during BA polymerization at high-temperatures, was studied experimentally and compared with that of secondary radicals.[29] These midchain radicals undergo β-scission reactions. Numerous experimental[19,30−41] and theoretical[15,42−48] investigations have pointed out that CTP reactions can strongly impact the overall rate of polymerization. As CTP reactions affect the molecular structure of the final polymer,[19,49] a better understanding of CTP reactions will enable optimizing polymerization processes and producing desired polymers.[15,50,51]

CTP and β-scission reactions in thermal polymerization of *n*-BA and *n*-butyl methacrylate (BMA) have been studied using nuclear magnetic resonance (NMR) spectroscopy and electrospray ionization/Fourier transform mass spectroscopy

Special Issue: Scott Fogler Festschrift

Received: October 18, 2014
Revised: December 18, 2014
Accepted: December 29, 2014
Published: December 29, 2014

DOI: 10.1021/ie504110n
Ind. Eng. Chem. Res. 2015, 54, 4148−4165

(ESI/FTMS).[15,49,52] NMR analysis of these polymers indicated the presence of end groups from CTP reactions at temperatures lower than 70 °C.[19,33,49] Experimental studies have shown the important role of intramolecular chain transfer and scission reactions in the reduction of dead-polymer average molecular weights and the enhancement of the overall rate of polymerization.[7,12,15,42] NMR and ESI/FTMS analyses of samples from spontaneous (no thermal initiator added) high-temperature homopolymerization of ethyl acrylate (EA) and *n*-BA have shown that different branch points are generated during the polymerization.[25] The pulsed-laser polymerization/size exclusion chromatography (PLP/SEC) method was used to study the kinetics of CTP reactions in the polymerization of alkyl acrylate.[42,53] While pulsed-laser polymerization (PLP) has been used to estimate the rate constants of propagation reactions (k_p) of monomers such as styrene[54] and methyl methacrylate (MMA),[55] and chain transfer reactions of *n*-butyl methacrylate (BMA),[56] a reproducible value of the propagation rate constant obtained using low laser pulse-repetition rates (<100 Hz) has not been reported for alkyl acrylates at temperatures above 30 °C. The molecular-weight distributions of PLP-generated polymers showed peak broadening at temperatures above 30 °C, which was attributed to the occurrence of both inter- and intramolecular CTP reactions.[33,57] However, high repetition rates have been applied to overcome the temperature restrictions.[58] At temperatures above 30 °C, intermolecular CTP reactions in free-radical polymerization of *n*-BA[15,19] and 2-ethylhexyl acrylate[49] have also been studied using NMR spectroscopy. While these analytical techniques have been very useful in characterizing acrylate polymers generated from thermal free-radical polymerizations, their use has not led to a conclusive determination of specific reaction mechanisms or estimation of individual reaction kinetic parameters.

Macroscopic kinetic models have been used extensively[59] to estimate the rate constants of initiation, propagation, chain transfer, and termination reactions in free-radical polymerization of acrylates, from polymer-sample measurements of monomer conversions and average molecular weights.[59,60] However, the accuracy of these estimated kinetic parameters depends on the accuracy of the assumed mechanistic model and measurements used in the estimation. Also, these models are incapable of conclusively determining mechanisms and molecular species involved.

Computational quantum chemistry methods have been used successfully to explore the mechanisms of free-radical reactions.[61−76] Specifically, DFT has been widely applied to calculate the rate constants of initiation, propagation, chain transfer, and termination reactions in free-radical polymerization of various monomers.[61−75] The forward and reverse reaction rate coefficients have been calculated for a series of reversible addition−fragmentation chain-transfer (RAFT) reactions using high-level wavefunction-based quantum chemistry calculations.[77] DFT-based methods are computationally less intensive than wavefunction-based methods,[78,79] and are therefore preferred for studying chain transfer reactions in the polymerization of alkyl acrylates given the large size of the polymer system. Molecular geometries and rate constants of various reactions in the polymerization of alkenes and acrylates have been predicted accurately using DFT-based methods.[62,69] The B3LYP/6-31G(d) level of theory has been applied to explore self-initiation mechanisms of styrene,[68] MA, EA, *n*-BA,[8,9] and MMA,[10] cyclohexanone-monomer co-initiation reaction in thermal homopolymerization of MA and MMA,[80] and propagation reactions of alkenes,[62,71] MA,[78] and MMA[81] in the gas phase. Chain transfer to monomer (CTM)[82] and chain transfer to solvent (CTS)[83] reactions have also been studied. Before this study, there was no report on the optimal level of theory needed to explore CTP reactions or dead polymer structures that most likely release a hydrogen atom during CTP reactions in high temperature polymerization of alkyl acrylates.

Solvent molecules are known to affect the stability of transition-state structures of reactions in solution free-radical polymerization.[84] The solvent stabilization of transition-state structures can cause significant differences between gas-phase rate constants calculated using computational quantum chemistry and rate constants obtained experimentally in solution polymerization.[85,86] The polarizable continuum model (PCM)[87,88] was applied to estimate the propagation rate coefficient of acrylic acid in the presence of toluene,[89] and small differences between gas-phase and liquid-phase activation energies and rate constants were observed. Another solvation model, the conductor-like screening model (COSMO),[90] was applied to explore the effect of solvents with different dielectric constants on the propagation rate coefficients in free-radical polymerization of acrylonitrile and vinyl chloride.[91] In addition, COSMO was applied to predict nonequilibrium solvation energies of biphenyl-cyclohexane-naphthalene.[92] The performances of PCM and COSMO in predicting solvent effects on kinetic parameters of CTS reactions have also been compared.[83] Integral equation formalism (IEF),[93,94] which is a version of PCM, was used to study polar interaction effects on barriers of chain transfer to several agents in free-radical polymerization of ethylene, MMA, and acrylamide based on integral operators.[95] In this work we apply IEF-PCM and COSMO to CTP reactions, compare the performances of IEF-PCM and COSMO, and determine the effects of several solvents on the reactions.

DFT has been applied to calculate the entropy change of various organic reactions, giving entropies that are in good agreement with experimental values.[96] This good agreement has also been reported for systems with high molecular weights.[96] However, large differences between the entropies of bimolecular and unimolecular reactions have been observed.[97] These differences have been blamed on the different degrees-of-freedom lost in these reactions.[97] In the unimolecular reactions, the net change in the number of degrees of translation, rotation, and vibration is zero. However, in bimolecular reactions, there is a loss of three translational and three rotational degrees of freedom (a gain of six new vibrational modes).[97] In bimolecular reactions, in which two species are interacting, the total entropy of the system is approximately the entropy of one of the species due to the large contribution of translational frequencies to the total entropy of the system.[11,96,97] The translational entropy of most molecules depends on the space available to the molecule (rather than mass of the molecule).[97] Temperature, moment of inertia, and the symmetry of a molecule play a major role in the calculation of the rotational entropy.[97] The vibrational entropy is proportional to the frequency of vibration and temperature.[97] Activation entropies of various bimolecular reactions have been reported[20,53,56,57,81,98] to be about −150 to −170 J mol^{-1} K^{-1}, which is higher (more negative) than those of unimolecular reactions.[97] Although entropies of transition states and reactants are lower in solution, the entropy change of dimerization of cyclopentadiene reaction in solution is only slightly different (13 J mol^{-1} K^{-1}) from that in the gas phase.[97] This has been attributed to the higher boiling

DOI: 10.1021/ie504110n
Ind. Eng. Chem. Res. 2015, 54, 4148−4165

point and consequently larger entropy of vaporization of the transition state than the reactants.[97,99]

In this work, mechanisms of CTP reactions in monomer self-initiated polymerization of alkyl acrylates are studied using DFT calculations. The mechanisms are investigated using three types of hybrid functionals (B3LYP, X3LYP, and M06-2X) and four basis sets (6-31G(d), 6-31G(d, p), 6-311G(d), and 6-311G(d, p)). Dead polymer chains with three different structures are considered. The CTP reactivities of MA, EA, and n-BA are calculated using these levels of theory, and the calculated values are compared with each other and experimental results. Two different implicit solvent models, IEF-PCM and COSMO, have been explored. The level of theory adequate for studying CTP reactions and proper solvent models to apply are investigated. The energy barrier and rate constant of each reaction are calculated using transition state theory and the rigid rotor harmonic oscillator (RRHO) approximation.

The rest of this paper is organized as follows. Section 2 discusses the applied computational methods. Section 3 provides results and discussion. Finally, section 4 presents concluding remarks.

2. COMPUTATIONAL METHODS

The thermodynamic and kinetic parameters (activation energies, enthalpies of reaction, Gibbs free energies, frequency factors, and rate constants) of intermolecular CTP reactions for MA, EA, and n-BA are calculated using DFT. Since there is exactly one unpaired spin in our systems, we use restricted open-shell wavefunctions in our calculations. B3LYP is selected to calculate energy barriers and optimize the molecular geometries of reactants, products, and transition states. X3LYP and M06-2X[100−102] functionals are applied to validate the calculated results. Four different basis sets (6-31G(d), 6-31G(d, p), 6-311G(d), and 6-311G(d, p)) are used with each of these functionals. Reactants and transition states are validated by performing Hessian calculations. NMR spectra of dead polymers generated by CTP mechanisms are calculated using several functionals (B3LYP, and X3LYP) and basis sets (6-31G(d), 6-31G(d, p), 6-311G(d), and 6-311G(d, p)). These calculated spectra are compared with experimental spectra reported for EA and n-BA polymers.[19,25] Implicit solvent models, IEF-PCM and COSMO, are applied to account for solvent effects. Minimum-energy pathways for several reactions of interest are determined using intrinsic reaction coordinated (IRC) calculations. Vibrational frequency scaling factors 0.960, 0.961, 0.966, and 0.967 are used for the B3LYP method with 6-31G(d), 6-31G(d,p), 6-311G(d), and 6-311G(d,p) basis sets, respectively. These scaling factors are from the National Institute of Standards and Technology (NIST) scientific and technical database.[103] We use GAMESS for all calculations.[104]

A rate constant $k(T)$ is calculated using the transition state theory[105] with

$$k(T) = (c^0)^{1-m}\frac{k_B T}{h}\exp\left(-\frac{\Delta H^{\ddagger} - T\Delta S^{\ddagger}}{RT}\right) \quad (1)$$

where c^0 is the inverse of the reference volume assumed in the translational partition function calculation, k_B is the Boltzmann constant, T is temperature, h is Planck's constant, R is the universal gas constant, m is the molecularity of the reaction, and $\Delta S^{\ddagger}$ and $\Delta H^{\ddagger}$ are the entropy and enthalpy of activation, respectively. $\Delta H^{\ddagger}$ is given by

$$\Delta H^{\ddagger} = E_0 + (\mathrm{ZPVE} + \Delta\Delta H)_{\mathrm{TS-R}} \quad (2)$$

where $\Delta\Delta H$ is the difference in enthalpy of the transition state (TS) and the reactants (R), ZPVE is the difference in zero-point vibrational energy between the transition state and the reactants, and E_0 is the barrier (the difference in electronic energy of the transition state and the reactants). In this work, the RRHO approximation[66,81] is used when estimating ZPVE, $\Delta\Delta H$, and $\Delta S^{\ddagger}$ due to its simplicity and reasonable accuracy shown in previous studies.[10,68,81] The activation energy (E_a) is calculated using

$$E_a = \Delta H^{\ddagger} + mRT \quad (3)$$

and the frequency factor (A) using

$$A = (c^0)^{1-m}\frac{k_B T}{h}\exp\left(\frac{mR + \Delta S^{\ddagger}}{R}\right) \quad (4)$$

Quantum tunneling should be considered in reactions involving the transfer of a hydrogen atom.[17,48,106,107] The Wigner tunneling[107] correction is calculated in this work using

$$\kappa \approx 1 + \frac{1}{24}\left(\frac{h\nu^{\ddagger}}{k_B T}\right)^2 \quad (5)$$

where $\nu^{\ddagger}$ is the imaginary frequency of the transition state.

3. RESULTS AND DISCUSSIONS

We consider three dead polymer structures formed by the three termination reactions shown in Figure 1. Two monoradicals can undergo termination by coupling reaction to form a dead polymer (D1) [Figure 1a]. A monoradical (M_1 shown in Figure 2) after one propagation step, can be terminated by hydrogen abstraction, leading to the formation of the dead polymer D2 [Figure 1b]. A monoradical with two monomer units can also react with a monoradical with one monomer unit to form a D3 dead polymer [Figure 1c].

3.1. Mechanisms of Chain Transfer to D1 Dead Polymer. Possible mechanisms of chain transfer to the D1 dead polymer for MA, EA, and n-BA, are shown in Figures 3, 4 and 5, respectively. The energy differences of optimized reactants and products involved in each of these mechanisms are calculated by applying B3LYP and X3LYP functionals and 6-31G(d), 6-31G(d,p), 6-311G(d), and 6-311G(d,p) basis sets. The results are reported in the Supporting Information (Tables S1, S2, and S3, respectively). These results indicate that MA2-D1-1, EA2-D1-1, and n-BA2-D1-1 mechanisms are exothermic, while the other mechanisms are endothermic. Since tertiary radicals are more stable than secondary radicals,[108,109] the likelihood of the occurrence of the MA2-D1-1, EA2-D1-1, and n-BA2-D1-1 mechanisms is higher.

The same functionals and basis sets are used to calculate the bond-dissociation energies of hydrogen atoms involved in the proposed mechanisms. These dissociation energies are given in Table 1. While in agreement with previous results,[102] they indicate that the bond-dissociation energies of hydrogen atoms attached to the tertiary carbon atoms (which are abstracted via MA2-D1-1, EA2-D1-1, and n-BA2-D1-1 mechanisms) are about 50 kJ/mol lower than those of other hydrogen atoms of the dead polymers. This suggests that such a tertiary carbon atom has a higher tendency to release a hydrogen atom.

3.1.1. Effect of the Type of the Radical that Initiated a Live MA-Polymer Chain. It has previously been reported[8,9] that two

DOI: 10.1021/ie504110n
Ind. Eng. Chem. Res. 2015, 54, 4148−4165

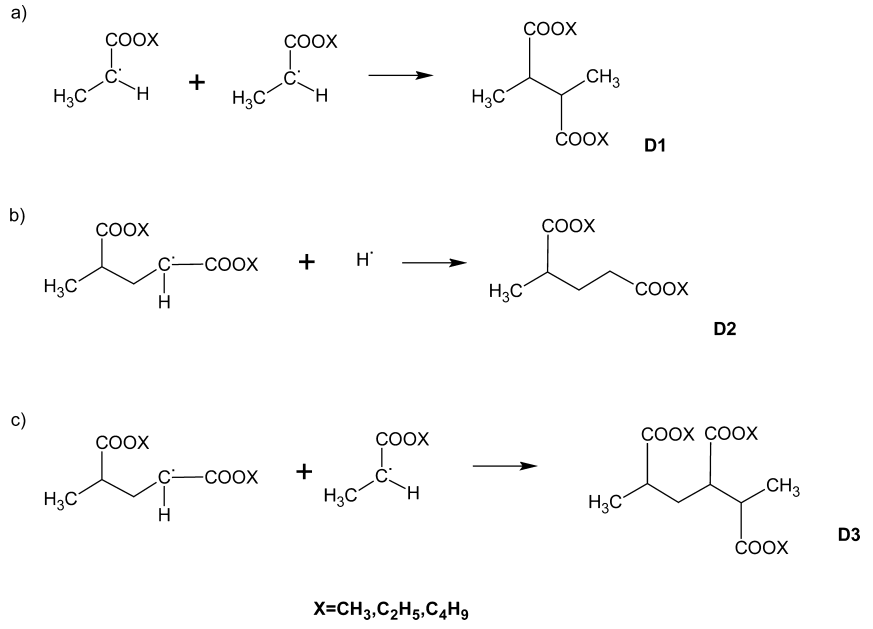

Figure 1. Dead polymer chains formed from (a) termination by coupling of two monoradicals, (b) termination by hydrogen abstraction, and (c) termination by coupling of a live chain and a monoradical.

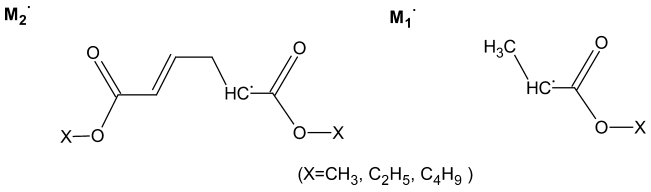

Figure 2. Two types of monoradicals generated by monomer self-initiation.[8,9]

types of monoradicals ($M_1^\bullet$ and $M_2^\bullet$) are produced in the monomer self-initiation of alkyl acrylates (Figure 2). The hydrogen atom abstraction from a tertiary carbon atom of a dead polymer chain initiated by $M_1^\bullet$ (MA1-D1-1, shown in Figure 6) and $M_2^\bullet$ (MA2-D1-1, shown in Figure 3) are investigated in this study. Three different functionals, B3LYP, X3LYP, and M06-2X, and several basis sets are applied. The MA1-D1-1 and MA2-D1-1 mechanisms are explored by sampling the potential energy surface with C1−H2 and H2−C3 bond lengths ranging from 1.19 to 1.59 Å. Figure 7a shows the transition-state geometry for the MA2-D1-1 mechanism with C1−H2 and H2−C3 bond lengths of 1.37 and 1.35 Å, respectively. The activation energies, enthalpies of activation, frequency factors, and rate constants of the MA2-D1-1 mechanism are provided in Table 2. These results show that the activation energies and rate constants calculated using different basis sets vary by ±10 kJ/mol and 2 orders of magnitude. The kinetic and thermodynamic parameters predicted using the M06-2X functional are different from those obtained with B3LYP and X3LYP (Table 2). It is important to note that the M06-2X functional is more accurate than the other functionals because it accounts for van der Waals (vdW) interactions.[110,111] B3LYP, as a hybrid GGA functional, depends on $\rho(r)$ and $|\nabla\rho(r)|$, where $\rho(r)$ is charge density at that point r. However, M06-2X is a hybrid meta-GGA functional and depends on $\rho(r)$, $|\nabla\rho(r)|$, and kinetic energy density. The rate constant estimates calculated

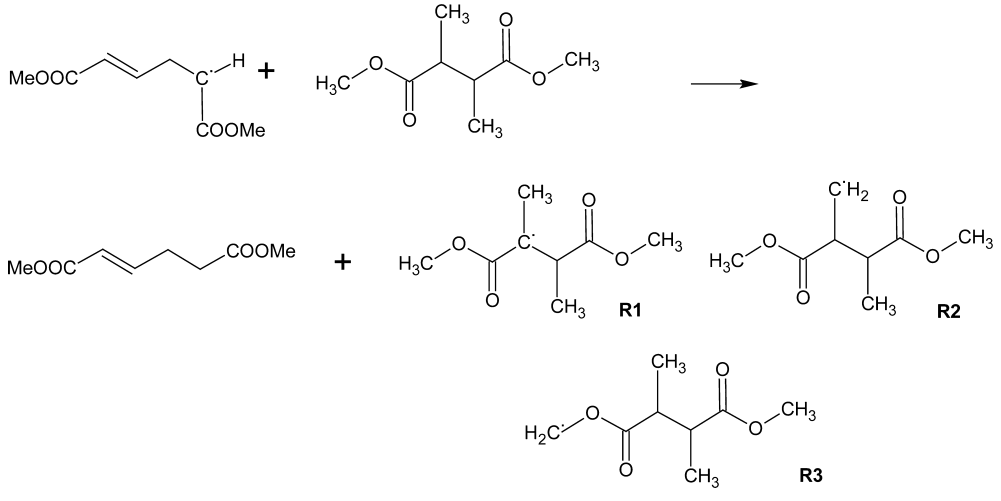

Figure 3. Possible chain transfer to polymer mechanisms for MA: Ri (i = 1, 2, and 3) is the radical formed through the MA2-D1-i mechanism.

DOI: 10.1021/ie504110n
Ind. Eng. Chem. Res. 2015, 54, 4148−4165

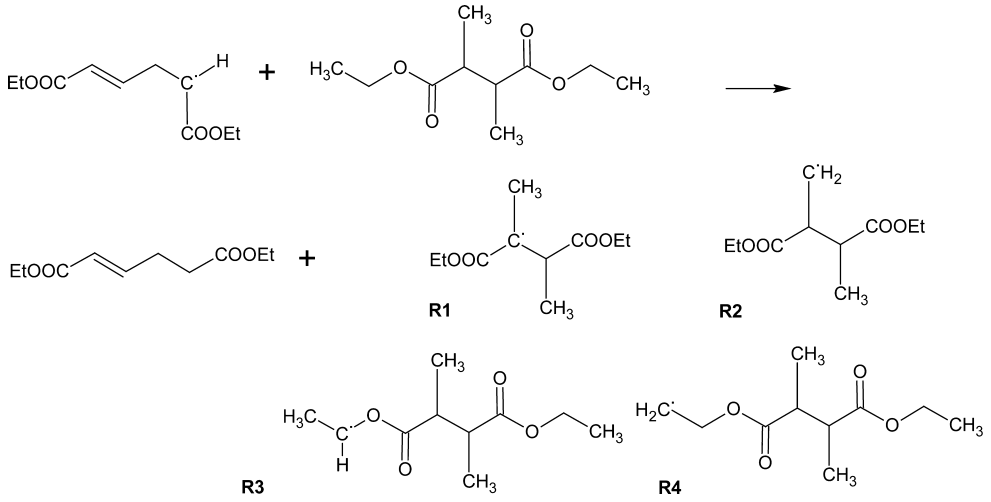

Figure 4. Possible chain transfer to polymer mechanisms for EA: R*i* (*i* = 1, 2, 3, and 4) is the radical formed through the EA2-D1-*i* mechanism.

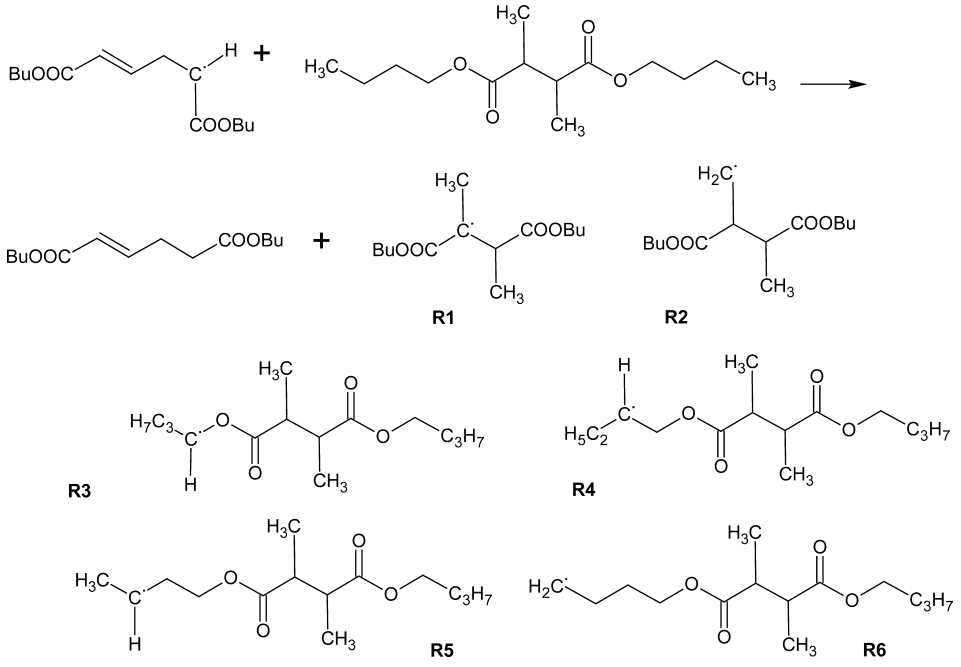

Figure 5. Possible chain transfer to polymer mechanisms for *n*-BA; R*i* (*i* = 1, 2, 3, 4, 5, and 6) is the radical formed through the *n*-BA2-D1-*i* mechanism.

Table 1. H−R Bond Dissociation Energies (kJ mol^{-1}) at 298 K

mechanism	B3LYP 6-31G(d)	B3LYP 6-31G(d,p)	B3LYP 6-311G(d)	B3LYP 6-311G(d,p)	X3LYP 6-31G(d)	X3LYP 6-31G(d,p)	X3LYP 6-311G(d)	X3LYP 6-311G(d,p)
MA2-D1-1	387	390	383	385	385	387	384	387
MA2-D1-2	446	448	440	441	447	450	441	443
MA2-D1-3	435	436	428	429	435	437	429	431
EA2-D1-1	387	390	383	385	388	391	385	387
EA2-D1-2	445	448	440	441	447	450	441	443
EA2-D1-3	422	424	417	419	423	425	418	420
EA2-D1-4	451	453	445	447	452	455	446	448
n-BA2-D1-1	387	390	383	385	388	392	385	387
n-BA2-D1-2	446	449	440	442	447	450	441	443
n-BA2-D1-3	422	424	417	418	423	426	418	419
n-BA2-D1-4	433	436	429	430	435	438	425	432
n-BA2-D1-5	429	432	424	426	431	434	425	427
n-BA2-D1-6	447	449	440	442	448	451	441	443

DOI: 10.1021/ie504110n
Ind. Eng. Chem. Res. 2015, 54, 4148−4165

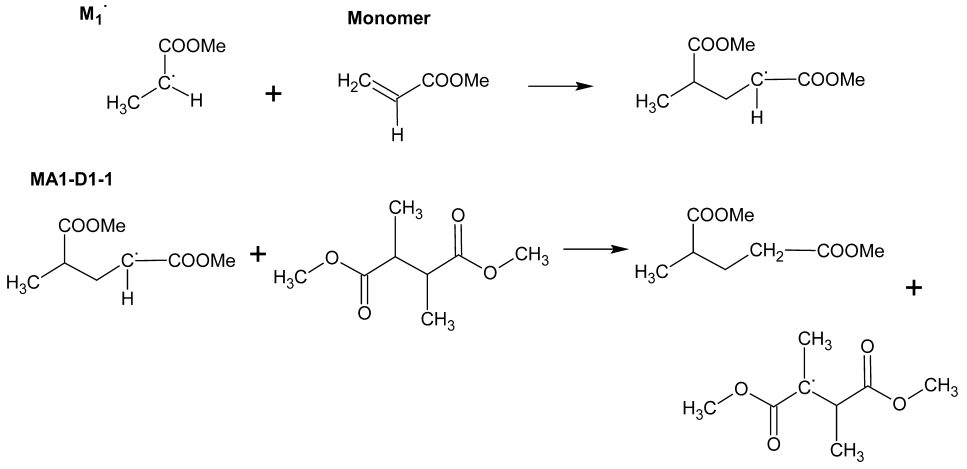

Figure 6. Most probable CTP mechanisms involving two-MA-unit live chain initiated by $M_1^{\bullet}$.

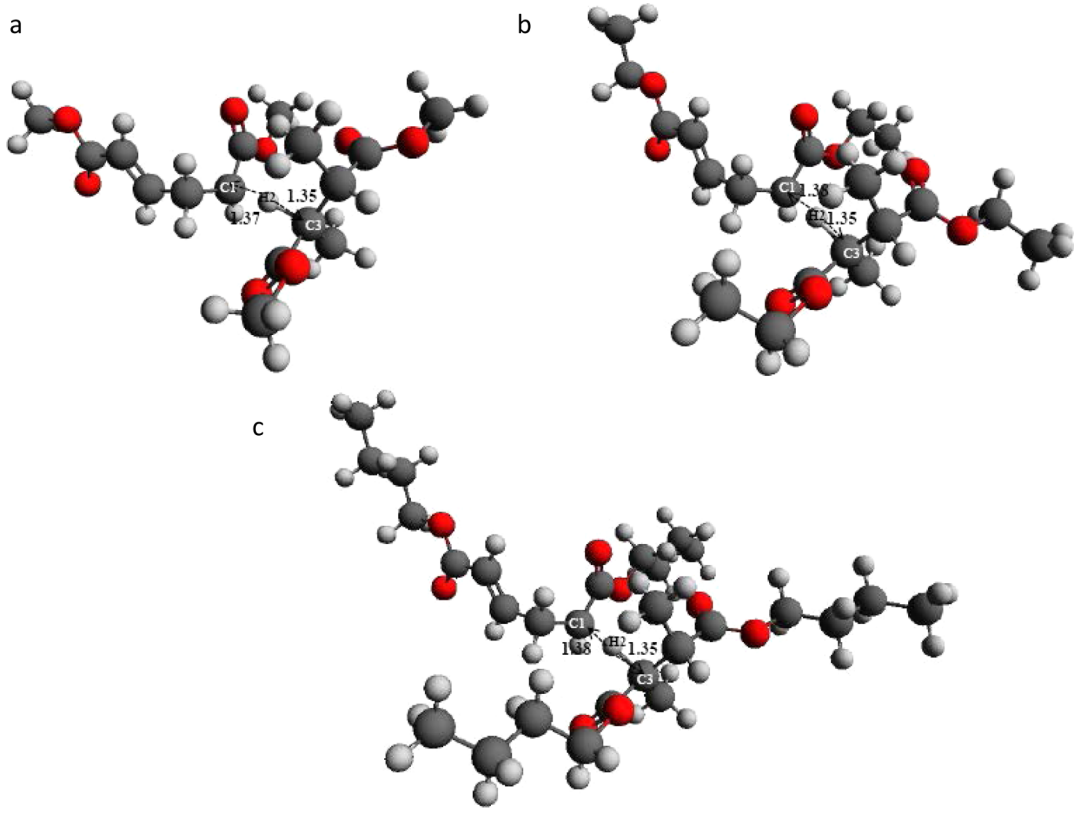

Figure 7. Transition state geometry for the MA2-D1-1 (a), EA2-D1-1 (b), and *n*-BA2-D1-1 (c) mechanisms.

using M06-2X are in good agreement with experimental values reported for CTM reactions of MA, EA, and *n*-BA.[82] No significant change in activation energies or rate constants was observed with different basis sets. The transition-state structure of the MA1-D1-1 mechanism has C1−H2 and H2−C3 bond lengths of 1.37 and 1.36 Å, respectively (Supporting Information, Figure S1). Table 2 gives the kinetic parameters for the MA1-D1-1 mechanism. A comparison of the activation energies and rate constants calculated for the MA2-D1-1 and MA1-D1-1 mechanisms indicates that the type of radical that initiated the live chain has little or no effect on the capability of the live chain to participate in a CTP reaction. However, as Table 2 shows that $M_2^{\bullet}$ is a little more reactive in MA CTP reactions than $M_1^{\bullet}$; for EA and *n*-BA we study hydrogen abstraction by a live polymer chain initiated by $M_2^{\bullet}$.

3.1.2. CTP Mechanisms for EA and n-BA. EA2-D1-1 (Figure 4) and *n*-BA2-D1-1 (Figure 5) CTP mechanisms are examined. The abstraction of a hydrogen atom from a tertiary carbon by a live polymer chain initiated by $M_2^{\bullet}$ is studied by choosing C1−H2 and H2−C3 bond lengths as reaction coordinates. The C1−H2 and H2−C3 bond lengths of the transition-state structure for the EA2-D1-1 mechanism are 1.38 and 1.35 Å, respectively (Figure 7b). The activation energies, enthalpies of reaction, frequency factors, and rate constants of the EA2-D1-1 mechanism are given in Table 3. The activation energies and rate constants calculated using the methods B3LYP and X3LYP

DOI: 10.1021/ie504110n
Ind. Eng. Chem. Res. 2015, 54, 4148−4165

Table 2. Activation Energy (E_a), Enthalpy of Activation ($\Delta H^{\ddagger}$), and Gibb's Free Energy of Activation ($\Delta G^{\ddagger}$) in kJ mol^{-1}; Tunneling Factor (κ_w for Wigner Correction); Frequency Factor (A) and Rate Constant (k, without Tunneling; and k_w, with Tunneling) in M^{-1} s^{-1}, for the Most Probable CTP Mechanisms for MA at 298 K; and Rate Constant without Tunneling at 413 K (k_{413})

	B3LYP 6-31G(d)	B3LYP 6-31G(d,p)	B3LYP 6-311G(d)	B3LYP 6-311G(d,p)	X3LYP 6-31G(d)	X3LYP 6-31G(d,p)	X3LYP 6-311G(d)	X3LYP 6-311G(d,p)	M06-2X 6-31G(d)	M06-2X 6-31G(d,p)	M06-2X 6-311G(d)	M06-2X 6-311G(d,p)
Hydrogen Abstraction via MA2-D1-1												
E_a	57	55	63	60	52	47	59	54	30	28	31	29
$\Delta H^{\ddagger}$	52	50	58	55	47	42	54	49	25	23	26	24
$\Delta G^{\ddagger}$	108	108	117	111	108	106	105	104	88	85	85	84
log $_eA$	12.08	11.32	11.17	12.16	10.16	8.76	14.17	12.39	9.29	9.56	10.97	10.67
k	1.6×10^{-5}	1.6×10^{-5}	5.4×10^{-7}	5.9×10^{-6}	2.0×10^{-5}	4.1×10^{-5}	5.5×10^{-5}	7.8×10^{-5}	5.8×10^{-2}	1.9×10^{-1}	1.9×10^{-1}	3.4×10^{-1}
κ_w	3.58	3.49	3.64	3.6	3.83	3.73	3.98	3.78	3.11	3.08	3.19	3.07
k_w	5.73×10^{-5}	5.58×10^{-5}	1.97×10^{-6}	2.12×10^{-5}	7.66×10^{-5}	1.53×10^{-4}	2.19×10^{-4}	2.95×10^{-4}	1.8×10^{-1}	5.85×10^{-1}	6.06×10^{-1}	1.04
k_{413}	9.9×10^{-4}	1.6×10^{-3}	3.3×10^{-5}	3.5×10^{-4}	1.3×10^{-3}	3.2×10^{-3}	2.6×10^{-3}	3.7×10^{-3}	2.08×10^{0}	1.1×10^{1}	8.1×10^{1}	1.9×10^{1}
Hydrogen Abstraction via MA1-D1-1												
E_a	62	61	68	64	56	53	63	57	34	28	33	29
$\Delta H^{\ddagger}$	57	56	63	59	51	49	58	52	29	23	28	24
$\Delta G^{\ddagger}$	116	115	123	118	111	107	109	106	84	87	88	87
log $_eA$	10.99	10.84	10.52	11.15	10.49	11.15	13.97	12.7	12.35	9.11	10.49	9.1
k	7.2×10^{-7}	1.1×10^{-6}	4.9×10^{-8}	3.8×10^{-7}	6.2×10^{-6}	2.9×10^{-5}	9.9×10^{-6}	3.3×10^{-5}	2.7×10^{-1}	9.6×10^{-2}	6.2×10^{-2}	8.9×10^{-2}
κ_w	3.79	3.70	3.93	3.73	3.84	3.75	3.94	3.79	3.15	3.11	3.23	3.18
k_w	2.73×10^{-6}	4.07×10^{-6}	1.93×10^{-7}	1.42×10^{-6}	2.38×10^{-5}	1.09×10^{-4}	3.9×10^{-5}	1.25×10^{-4}	8.5×10^{-1}	2.99×10^{-1}	2.00×10^{-1}	2.83×10^{-1}
k_{413}	3.7×10^{-5}	7.5×10^{-5}	2.2×10^{-6}	1.6×10^{-5}	2.8×10^{-4}	2.0×10^{-3}	2.5×10^{-4}	2.6×10^{-3}	1.9×10^{0}	4.7×10^{0}	3.1×10^{0}	3.5×10^{0}

Ind. Eng. Chem. Res. 2015, 54, 4148−4165 DOI: 10.1021/ie504110n

Table 3. Activation Energy (E_a), Enthalpy of Activation ($\Delta H^{\ddagger}$), and Gibb's Free Energy of Activation ($\Delta G^{\ddagger}$) in kJ mol^{-1}; Tunneling Factor (κ_w for Wigner Correction); Frequency Factor (A) and Rate Constant (k, without Tunneling; and k_w, with Tunneling) in M^{-1} s^{-1}, for the Most Probable CTP Mechanism for EA (EA2-D1-1) at 298 K; and Rate Constant without Tunneling at 413 K (k_{413})

	B3LYP 6-31G(d)	B3LYP 6-31G(d,p)	B3LYP 6-311G(d)	B3LYP 6-311G(d,p)	X3LYP 6-31G(d)	X3LYP 6-31G(d,p)	X3LYP 6-311G(d)	X3LYP 6-311G(d,p)	M06-2X 6-31G(d)	M06-2X 6-31G(d,p)	M06-2X 6-311G(d)	M06-2X 6-311G(d,p)
E_a	59	56	66	63	54	49	62	59	24	21	24	23
$\Delta H^{\ddagger}$	54	51	61	58	49	44	57	54	19	16	19	19
$\Delta G^{\ddagger}$	110	107	116	113	101	102	104	101	83	81	84	83
log $_eA$	11.96	12.22	12.31	12.39	13.81	11.35	15.61	15.51	8.71	8.7	8.6	8.7
k	8.4×10^{-6}	2.8×10^{-5}	6.4×10^{-7}	2.5×10^{-6}	3.2×10^{-4}	1.9×10^{-4}	8.5×10^{-5}	2.7×10^{-4}	4.2	1.1	3.2×10^{-1}	4.5×10^{-1}
κ_w	3.66	3.59	3.80	3.78	3.86	3.76	4.00	3.80	3.15	3.12	3.23	3.16
k_w	3.07×10^{-5}	1.0×10^{-4}	2.43×10^{-6}	9.45×10^{-6}	1.24×10^{-3}	7.14×10^{-4}	3.4×10^{-4}	1.03×10^{-3}	1.32×10^{1}	3.43	1.03	1.42
k_{413}	1.4×10^{-3}	5.9×10^{-3}	9.6×10^{-5}	7.0×10^{-4}	5.1×10^{-2}	3.3×10^{-2}	1.4×10^{-2}	2.7×10^{-2}	7.1×10^{1}	1.3×10^{2}	4.6×10^{1}	5.3×10^{1}

and the basis sets (6-31G(d), 6-31G(d,p), 6-311G(d), and 6-311G(d,p)) are different at most by 13 kJ/mol and 2 orders of magnitude. The performance of M06-2X with different basis sets is more consistent: the difference in activation energies is within 3 kJ/mol and rate constants within 1 order of magnitude. The transition-state structure of the *n*-BA2-D1-1 mechanism is shown in Figure 7c, and the kinetic parameter values are given in Table 4. Our finding that *n*-BA2-D1-1 is the most probable mechanism of CTP is in agreement with previous studies.[42] Our calculated activation energy, using B3LYP/6-31G(d,p), is about 20 kJ/mol higher than a reported experimental value of 29 kJ/mol,[42] and our calculated rate constant (7.4×10^{-06}) is lower by about 4 orders of magnitude.[42] This indicates that the level of theory applied is adequate to accurately predict the mechanistic pathway and transition state structures but not the kinetics of the reaction. This inadequacy is attributed to the limitation of the hybrid functionals and the use of RRHO. First-principles DFT that only assumes the nonrelativistic Schrodinger equation is a powerful tool to directly study the mechanism and kinetics of each individual reaction in free-radical polymerization. Although discrepancies between DFT-calculated and experimentally determined activation energies and frequency factors have been reported, previous studies have shown that DFT is a reliable approach for estimating rate constants in free-radical polymerization,[11,20,21,82,112] due to error cancellation in electronic structure (activation energy) and entropy (frequency factor) calculations (under- or overestimation of both the activation energy and frequency factor leading to self-canceling errors) when studying liquid-phase reactions.[113] The accuracy of DFT depends on the approximation of exchange-correlation functionals which can be classified based on their functional form.[114−116] Local functionals (depending only on charge density $\rho(r)$ at that point r), generalized gradient-approximation (GGA) (depending on $\rho(r)$ and $|\nabla\rho(r)|$), and meta-GGA functionals (depending on $\rho(r)$, $|\nabla\rho(r)|$, and kinetic energy density) can be combined with Hartree−Fock exchange functionals to increase accuracy (which are known as hybrid functionals). For example, B3LYP, which is a hybrid GGA functional, has been used extensively due to its attractive performance-to-cost ratio.[8,9] Meta-GGA and hybrid meta-GGA functionals such as M06-2X provide a more accurate prediction of barrier heights, as they can adequately account for van der Waals interactions.[100−102,110,111] Further investigation with higher levels of theory such as G4 is needed.

Table 4. Activation Energy (E_a), Enthalpy of Activation ($\Delta H^{\ddagger}$), and Gibb's Free Energy of Activation ($\Delta G^{\ddagger}$) in kJ mol^{-1}; Tunneling Factor (κ_w for Wigner Correction); Frequency Factor (A) and Rate Constant (k, without Tunneling; and k_w, with Tunneling) in M^{-1} s^{-1}, for the *n*-BA2-D1-1 Mechanism at 298 K; and Rate Constant without Tunneling at 413 K (k_{413})

	B3LYP/6-31G(d)	B3LYP/6-31G(d,p)
E_a	56	53
$\Delta H^{\ddagger}$	51	48
$\Delta G^{\ddagger}$	114	110
log $_eA$	9.27	9.71
k	1.70×10^{-6}	7.40×10^{-6}
κ_w	3.75	3.68
k_w	6.37×10^{-6}	2.72×10^{-5}
k_{413}	1.30×10^{-3}	4.50×10^{-3}

DOI: 10.1021/ie504110n
Ind. Eng. Chem. Res. 2015, 54, 4148−4165

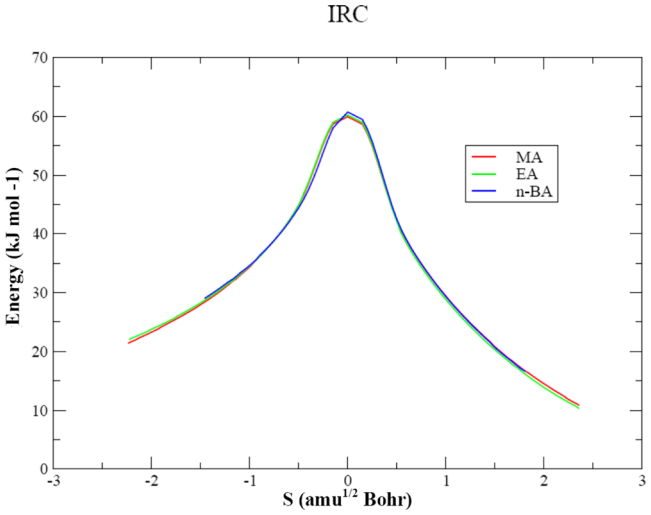

Figure 8. Intrinsic reaction coordinate (IRC) paths for the MA2-D1-1, EA2-D1-1, and *n*-BA2-D1-1 mechanisms (energies are relative to reactants).

The kinetic parameters estimated for the most likely CTP mechanisms of MA, EA, and *n*-BA (MA2-D1-1, EA2-D1-1, and *n*-BA2-D1-1) indicate that the end-substituent groups (methyl, ethyl, and butyl acrylate side chains) do not affect the kinetics of CTP reaction in the alkyl acrylates. This can be explained through the similarity of the reactive sites involved in the CTP reaction of MA, EA, and *n*-BA.[82,83] The pathways for the CTP mechanisms in the alkyl acrylates (MA2-D1-1, EA2-D1-1, and *n*-BA2-D1-1) are determined through IRC calculations (Figure 8). The presence of concerted pathways can be observed through these calculations in the forward and backward directions starting from transition-state structures for MA, EA, and *n*-BA.

3.1.3. Effect of the Live Polymer Chain Length. The effects of the length of a live polymer chain on the activation energies and the geometries of transition states are explored for MA and EA. The abstraction a hydrogen atom from a dead polymer chain by a live chain, which is initiated by $M_2^{\bullet}$ and has 3 or 4 monomer units, is investigated for MA (Figure 9). The activation energies and rate constants of these mechanisms are given in Table 5. They indicate that the rate constants change at most 2 orders of magnitude, as the length of the live chain changes. The activation energies of these reactions nearly do not change (at most 4 kJ/mol) by increasing the length of the live chain.

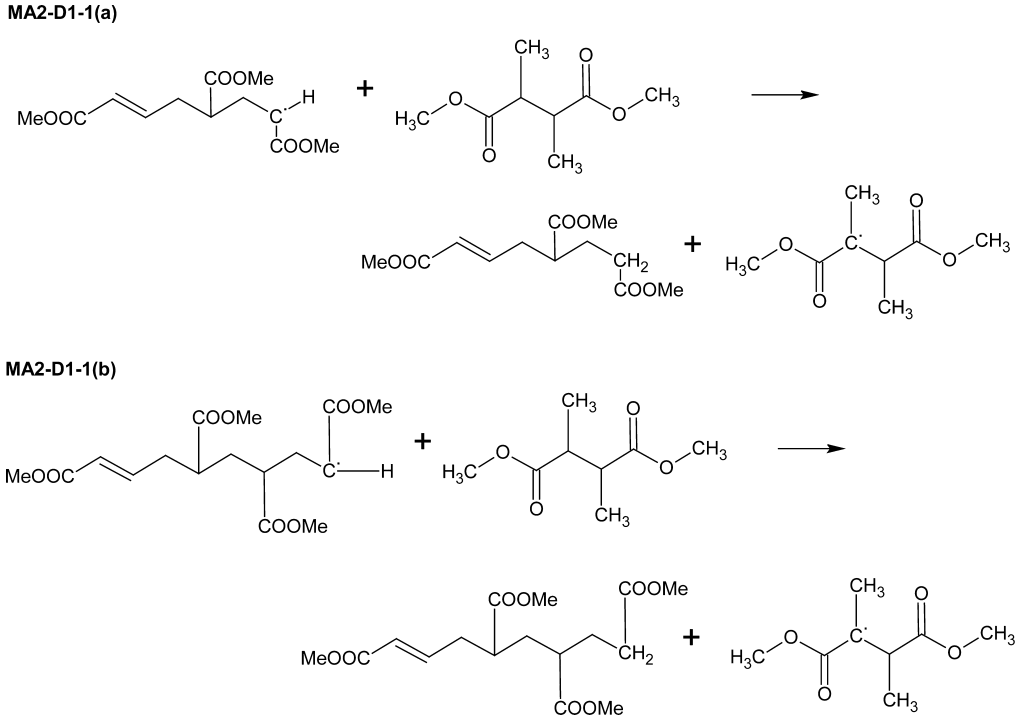

Figure 9. Most probable CTP mechanism involving a three [MA2-D1-1(a)] or four [MA2-D1-1(b)] MA-unit live chain initiated by $M_2^{\bullet}$.

Table 5. Bond Length in Å, Activation Energy (E_a), Enthalpy ($\Delta H^{\ddagger}$), and Free Energy ($\Delta G^{\ddagger}$) in kJ mol^{-1}; Tunneling Factor (κ_w for Wigner Correction); and Frequency Factor (A) and Rate Constant (k, without Tunneling; and k_w: with Tunneling) in M^{-1} s^{-1} by Considering the Radicals with Different Monomer Units for MA and EA, Using B3LYP/6-31G(d,p)

(C1−H2) Å	(C3−H2) Å	E_a	$\Delta H^{\ddagger}$	$\Delta G^{\ddagger}$	log $_eA$	k	κ_w	k_w
MA2-D1-1 Three Monomer Units								
1.37	1.35	59	54	114	10.63	1.70×10^{-6}	3.76	6.39×10^{-6}
MA2-D1-1 Four Monomer Units								
1.39	1.36	56	51	118	7.56	3.00×10^{-7}	3.86	1.16×10^{-6}
EA2-D1-1 Three Monomer Units								
1.37	1.36	54	49	123	4.52	3.80×10^{-8}	3.79	1.44×10^{-7}

DOI: 10.1021/ie504110n
Ind. Eng. Chem. Res. 2015, 54, 4148−4165

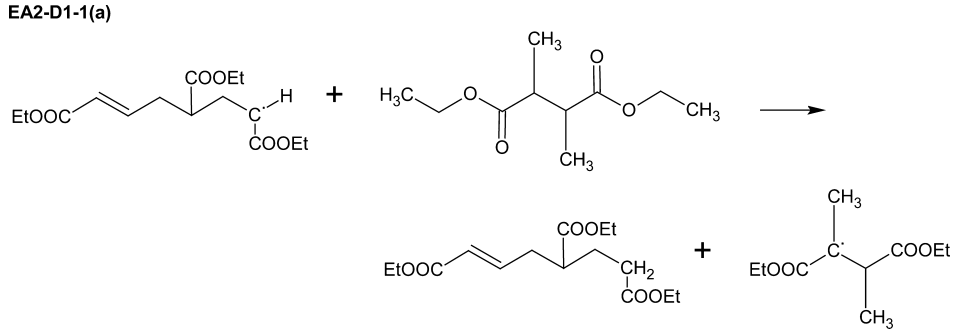

Figure 10. Most probable CTP mechanism involving a three EA-unit live chain initiated by $M_2^{\bullet}$.

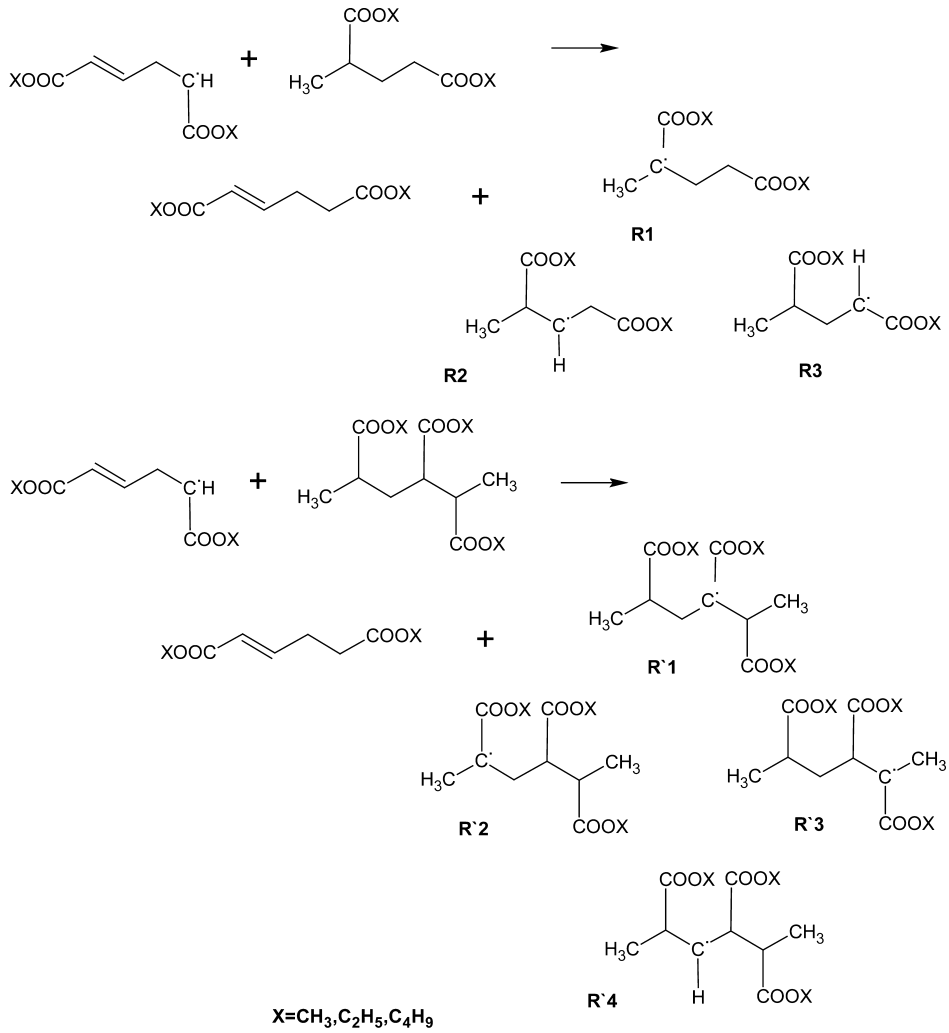

Figure 11. Possible chain transfer to the D2 and D3 dead polymers mechanisms for MA, EA, and *n*-BA; R*i* (*i* = 1, 2, and 3) and R'*i* (*i* = 1, 2, 3, and 4) are the radicals formed through the Y-D2-*i* and Y-D3-*i* mechanisms, respectively; Y= MA, EA, and *n*-BA.

Table 6. H−R Bond Dissociation Energies (kJ mol^{-1}) for D2 and D3 Dead Polymers at 298 K, Using B3LYP/6-31G(*d,p*)

H−R bond-dissociation energy						
Y-D2-1	Y-D2-2	Y-D2-3	Y-D3-1	Y-D3-2	Y-D3-3	Y-D3-4
363	417	387	357	364	366	405

The mechanism of CTP for EA (EA2-D1-1(a)) is explored as shown in Figure 10. In this mechanism the live chain has three monomer units. The activation energy and rate constant of EA2-D1-1 (including two monomer units) mechanism do not change significantly, as the length of the live polymer chain increases (Table 5). This agrees with previous theoretical studies that the propagation rate constants of MA and MMA are insensitive to the chain length after the first propagating step.[81] Such chain-length insensitivity has also been reported for homotermination rate coefficients in free-radical polymerization of acrylates.[117] These findings indicate that it is appropriate to use a dimer (trimer) model system to study the chain transfer to polymer reaction.

DOI: 10.1021/ie504110n
Ind. Eng. Chem. Res. 2015, 54, 4148−4165

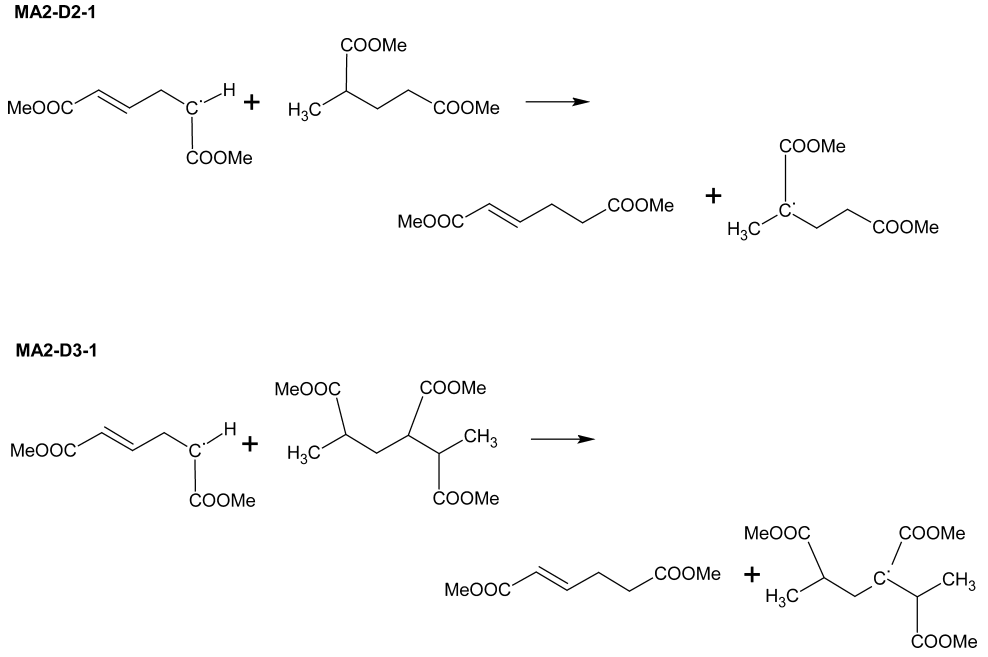

Figure 12. Most probable CTP mechanism involving a two MA-unit live chain initiated by $M_2^{\bullet}$.

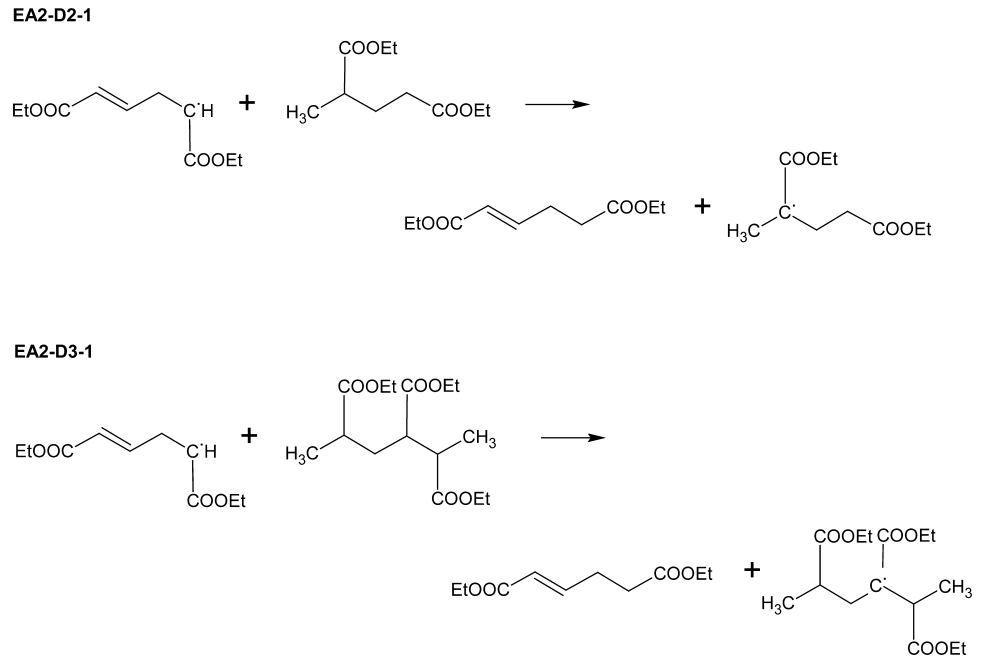

Figure 13. Most probable CTP mechanism involving a two EA-unit live chain initiated by $M_2^{\bullet}$.

3.2. Chain Transfer to D2 and D3 Dead Polymers. Live polymer chains can also abstract a hydrogen atom from these dead polymers (D2 and D3). B3LYP/6-31G(*d,p*) functional is used to calculate the bond-dissociation energies of hydrogen atoms in D2 and D3 dead polymers which are abstracted by a live polymer chain (Figure 11). The bond energies are reported in Table 6. These results indicate that those hydrogen atoms being abstracted via Y-D2-1 and Y-D3-1 mechanisms are the most labile ones for abstraction. The most probable mechanisms of chain transfer to D2 and D3 dead polymers are shown for MA (Figure 12), EA (Figure 13), and *n*-BA (Figure 14). Table 7 gives the kinetic parameters of these mechanisms for MA, using B3LYP and M06-2X (6-31G(*d,p*), 6-311G(*d*), and 6-311G(*d,p*)) functionals. A comparison of these results with those obtained for chain transfer to D1 dead polymer of MA, using B3LYP functional, indicates that the rate constant of the MA2-D2-1 mechanism is about 3 orders of magnitude higher than that calculated for MA2-D1-1, and its energy barrier is lower by about 6 kJ/mol. Although using M06-2X functional shows the same difference in the rate constants of MA2-D1-1 and MA2-D2-1 (3 orders of magnitude), it results in a much lower difference in energy barriers. The geometries of transition-state structures of MA2-D2-1 and MA2-D3-1 mechanisms are shown in Figure 15.

DOI: 10.1021/ie504110n
Ind. Eng. Chem. Res. 2015, 54, 4148−4165

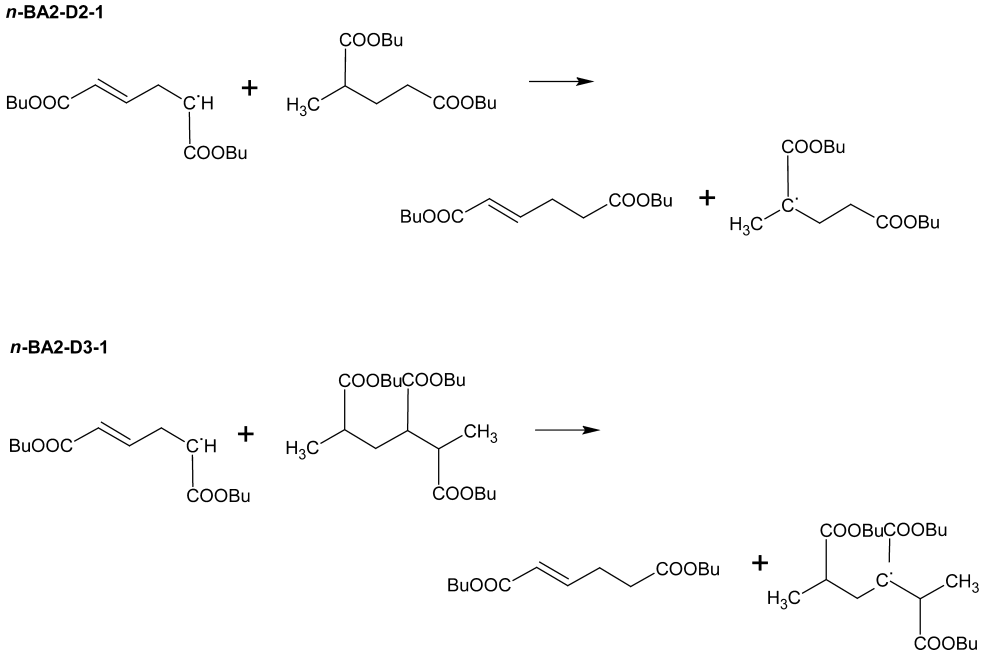

Figure 14. Most probable CTP mechanism involving a two *n*-BA-unit live chain initiated by $M_2^{\bullet}$.

Table 7. Activation Energy (E_a), Enthalpy of Activation ($\Delta H^{\ddagger}$), and Gibb's Free Energy of Activation ($\Delta G^{\ddagger}$) in kJ mol^{-1}; Tunneling Factor (κ_w for Wigner Correction); and Frequency Factor (A) and Rate Constant (k, without Tunneling; k_w: with Tunneling) in M^{-1} s^{-1} for the MA2-D2-1 and MA2-D3-1 Mechanisms at 298 K; and Rate Constant without Tunneling at 413 K (k_{413})

	B3LYP/6-31G(d,p)	B3LYP/6-311(d)	B3LYP/6-311G(d,p)	M06-2X/6-31G(d,p)	M06-2X/6-311(p)	M06-2X/6-311G(d,p)
			Hydrogen Abstraction via MA2-D2-1			
E_a	49	56	53	27	30	28
$\Delta H^{\ddagger}$	44	51	48	22	25	23
$\Delta G^{\ddagger}$	92	97	95	67	72	71
log $_eA$	15.31	15.74	15.73	16.38	15.65	15.53
k	1.07×10^{-2}	1.26×10^{-3}	4.07×10^{-3}	2.36×10^{2}	3.69×10^{1}	6.52×10^{1}
κ_w	3.44	3.68	3.66	2.98	3.11	2.97
k_w	3.68×10^{-2}	4.63×10^{-3}	1.49×10^{-2}	7.03×10^{2}	1.15×10^{2}	1.94×10^{2}
k_{413}	4.3×10^{-1}	5.3×10^{-2}	2.2×10^{-1}	5.9×10^{3}	1.7×10^{3}	2.1×10^{3}
			Hydrogen Abstraction via MA2-D3-1			
E_a	62	69	66	23	26	24
$\Delta H^{\ddagger}$	57	64	61	18	21	19
$\Delta G^{\ddagger}$	112	118	116	86	88	88
log $_eA$	12.32	12.78	12.34	7.47	7.51	6.58
k	3.18×10^{-6}	3.34×10^{-7}	6.38×10^{-7}	1.47×10^{-1}	5.74×10^{-2}	6.18×10^{-2}
κ_w	3.85	4.13	3.93	3.32	3.42	3.29
k_w	1.22×10^{-5}	1.38×10^{-6}	2.51×10^{-6}	4.88×10^{-1}	1.96×10^{-1}	2.03×10^{-1}
k_{413}	2.3×10^{-4}	1.9×10^{-5}	3.2×10^{-5}	6.0×10^{0}	2.9×10^{0}	3.3×10^{0}

We apply the B3LYP functional to explore the same mechanisms for EA (EA2-D2-1 and EA2-D3-1) and *n*-BA (*n*-BA2-D2-1 and *n*-BA2-D3-1). The geometries of the transition-state structures of EA2-D2-1 and EA2-D3-1 mechanisms are shown in Figure 16. The activation energies and rate constants of the most probable chain transfer to D2 and D3 dead polymers of EA and *n*-BA are provided in Table 8. These results indicate that the activation energies of EA2-D2-1 and *n*-BA2-D2-1 mechanisms are lower than those of EA2-D1-1, EA2-D3-1, *n*-BA2-D1-1, and *n*-BA2-D3-1 mechanisms. These studies point to the higher reactivity of D2 to undergo CTP reactions (relative to D1 and D3).

3.3. Continuum Solvation Models: IEF-PCM and COSMO. The solvent effects on the kinetics of the most likely CTP mechanisms identified with gas-phase calculations are studied using two different solvation models, IEF-PCM and COSMO, and in two types of solvents, *n*-butanol and *p*-xylene. As shown in Table 9, the application of IEF-PCM, using B3LYP and M06-2X functionals (6-31G(*d,p*) and 6-311G(*d,p*) basis sets), shows strong solvent effects on the activation energy and rate constant of CTP reactions of the alkyl acrylates in *n*-butanol but weakly affects those in *p*-xylene, compared to gas-phase values. The IEF-PCM-calculated activation energies in *n*-butanol are higher than those obtained via gas-phase

DOI: 10.1021/ie504110n
Ind. Eng. Chem. Res. 2015, 54, 4148−4165

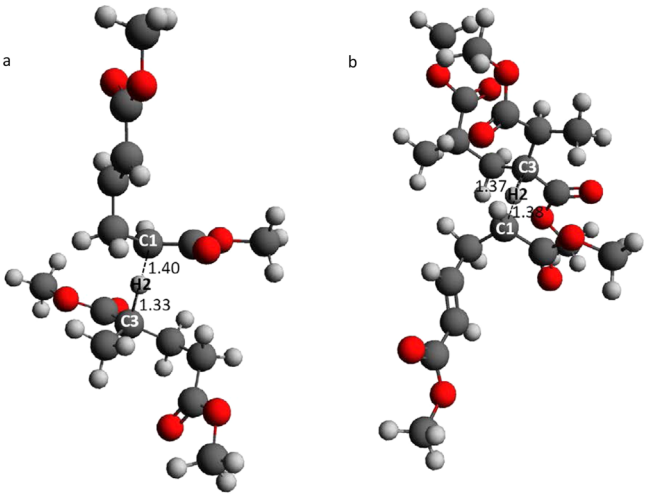

Figure 15. Transition state geometry for the MA2-D2-1 (a) and MA2-D3-1 (b) mechanisms.

calculations, resulting in lower rate constants. IEF-PCM calculations are further carried out to study CTP mechanisms for EA and *n*-BA, using B3LYP/6-31G(*d*) and 6-31G(*d,p*) (Table 10). Again, the application of IEF-PCM shows strong solvent effects on the activation energies and rate constants of CTP reactions in *n*-butanol, while its impact on the kinetic parameters of the reactions in *p*-xylene is negligible. Moreover, Tables 9 and 10 suggest that the effects that IEF-PCM predicts do not depend on the end substituent group. The reduction in the rate of the CTP reactions in *n*-butanol agrees with the "inhibiting effect" of *n*-butanol reported by Liang et al.,[118] who investigated the effect of *n*-butanol on the rate of intramolecular chain transfer to polymer reactions. They reported that *n*-butanol inhibits backbiting reactions and consequently reduces the rate of branching during the polymerization of *n*-BA and increases the average molecular weights of the polymer product.

However, as shown in Tables 9 and 10, the application of COSMO does not result in significant change of the (gas-phase-calculated) kinetic parameters of CTP reactions in *n*-butanol and *p*-xylene. The insignificant effects of COSMO on CTP reactions are in agreement with previous theoretical results reported for CTS reactions of acrylates[83] and propagation reactions of acrylonitrile and vinyl chloride.[91] On the basis of these results, we suggest that the IEF-PCM is a more appropriate solvation model for studying the free-radical polymerization of acrylates than COSMO.

4. CONCLUDING REMARKS

The mechanisms of intermolecular CTP reactions in self-initiated high-temperature polymerization of alkyl acrylates were studied theoretically. The abstraction of a hydrogen atom

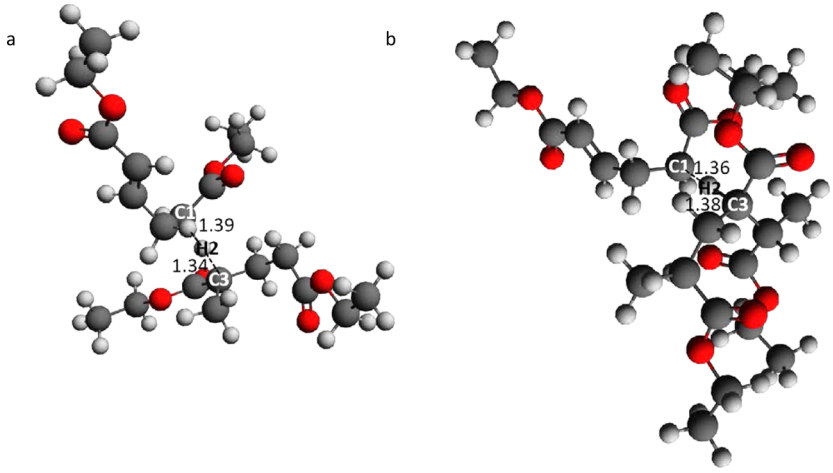

Figure 16. Transition state geometry for the EA2-D2-1 (a) and EA2-D3-1 (b) mechanisms.

Table 8. Activation Energy (E_a), Enthalpy of Activation ($\Delta H^{\ddagger}$), and Gibb's Free Energy of Activation ($\Delta G^{\ddagger}$) in kJ mol^{-1}; Tunneling Factor (κ_w for Wigner Correction); and Frequency Factor (A) and Rate Constant (k, without Tunneling; and k_w: with Tunneling) in M^{-1} s^{-1} for the Most Probable Mechanisms of Chain Transfer to D2 and D3 Dead Polymers of EA and *n*-BA at 298 K

	B3LYP/6-31G(d)		B3LYP/6-31G(d,p)		B3LYP/6-31G(d)	
	EA2-D2-1	EA2-D3-1	EA2-D2-1	EA2-D3-1	*n*-BA2-D2-1	*n*-BA2-D3-1
E_a	52	63	49	60	49	60
$\Delta H^{\ddagger}$	47	58	44	55	44	55
$\Delta G^{\ddagger}$	98	111	95	108	102	115
log $_eA$	13.21	12.53	14.19	13.56	11.19	10.5
k	4.19×10^{-4}	2.5×10^{-6}	3.49×10^{-3}	1.95×10^{-5}	1.86×10^{-4}	1.1×10^{-6}
κ_w	3.46	3.90	3.51	3.93	3.95	4.24
k_w	1.45×10^{-3}	9.75×10^{-6}	1.22×10^{-2}	7.66×10^{-5}	7.35×10^{-4}	4.66×10^{-6}
k_{413}	5.3×10^{-2}	1.1×10^{-4}	4.8×10^{-1}	3.1×10^{-3}	2.6×10^{-2}	6.3×10^{-4}

DOI: 10.1021/ie504110n
Ind. Eng. Chem. Res. 2015, 54, 4148−4165

Table 9. Activation Energy (E_a), Enthalpy of Activation ($\Delta H^{\ddagger}$), and Gibb's Free Energy of Activation ($\Delta G^{\ddagger}$) in kJ mol^{-1}; and Frequency Factor (A) and Rate Constant (k) in M^{-1} s^{-1} for the Most Probable CTP Mechanisms for MA at 298 K, Calculated Using IEF-PCM and COSMO

	hydrogen abstraction via MA2-D2-1				hydrogen abstraction via MA2-D3-1			
	B3LYP 6-31G(d,p)	B3LYP 6-311G(d,p)	M06-2X 6-31G(d,p)	M06-2X 6-311G(d,p)	B3LYP 6-31G(d,p)	B3LYP 6-311G(d,p)	M06-2X 6-31G(d,p)	M06-2X 6-311G(d,p)
IEF-PCM								
p-xylene								
E_a	53	55	30	31	64	67	24	26
$\Delta H^{\ddagger}$	48	50	25	26	59	62	19	21
$\Delta G^{\ddagger}$	97	98	82	85	116	119	88	92
log $_eA$	14.94	15.30	11.81	10.73	11.45	11.69	6.88	6.04
k	1.55×10^{-3}	1.01×10^{-3}	7.4×10^{-1}	1.68×10^{-1}	5.69×10^{-7}	2.16×10^{-7}	6.04×10^{-2}	1.16×10^{-2}
n-butanol								
E_a	56	59	34	36	70	75	31	33
$\Delta H^{\ddagger}$	51	54	29	31	65	70	26	28
$\Delta G^{\ddagger}$	105	104	87	92	125	128	98	102
log $_eA$	13.08	14.21	11.09	9.88	10.49	11.09	5.44	4.84
k	6.8×10^{-5}	6.81×10^{-5}	7.2×10^{-2}	9.60×10^{-3}	1.93×10^{-8}	4.68×10^{-9}	8.50×10^{-4}	2.07×10^{-4}
COSMO								
p-xylene								
E_a	49	52	24	25	57	60	23	25
$\Delta H^{\ddagger}$	44	47	19	20	52	55	18	20
$\Delta G^{\ddagger}$	94	99	78	79	109	113	87	88
log $_eA$	14.61	13.62	11.12	10.61	11.81	11.21	6.76	7.12
k	5.37×10^{-3}	6.29×10^{-4}	3.34	1.68	1.38×10^{-5}	2.25×10^{-6}	7.2×10^{-2}	5.1×10^{-2}
n-butanol								
E_a	50	51	24	25	56	59	23	24
$\Delta H^{\ddagger}$	45	46	19	20	51	54	18	19
$\Delta G^{\ddagger}$	95	97	78	79	107	111	87	86
log $_eA$	14.62	13.86	11.12	10.13	11.93	11.57	6.76	7.72
k	5.4×10^{-3}	1.2×10^{-3}	3.34	1.56	2.32×10^{-5}	4.8×10^{-6}	7.3×10^{-2}	1.4×10^{-1}

Table 10. Activation Energy (E_a), Enthalpy of Activation ($\Delta H^{\ddagger}$), and Gibb's Free Energy of Activation ($\Delta G^{\ddagger}$) in kJ mol^{-1}; and Frequency Factor (A) and Rate Constant (k) in M^{-1} s^{-1} for the Most Probable CTP Mechanisms for EA and *n*-BA at 298 K, Calculated Using COSMO and IEF-PCM

	B3LYP/6-31G(d,p)		B3LYP/6-31G(d,p)		B3LYP/6-31G(d)	
	EA2-D2-1	EA2-D3-1	EA2-D2-1	EA2-D3-1	*n*-BA2-D2-1	*n*-BA2-D3-1
COSMO						
E_a	50	62	49	61	48	57
$\Delta H^{\ddagger}$	45	57	44	56	43	52
$\Delta G^{\ddagger}$	98	112	96	109	100	111
log $_eA$	13.13	12.65	13.50	13.38	11.81	10.73
k	8.7×10^{-4}	4.25×10^{-6}	1.87×10^{-3}	1.31×10^{-5}	5.20×10^{-4}	4.66×10^{-6}
IEF-PCM						
E_a	60	70	56	69	57	65
$\Delta H^{\ddagger}$	55	65	52	64	52	60
$\Delta G^{\ddagger}$	113	125	111	125	115	125
log $_eA$	11.09	10.61	10.73	10.01	9.17	8.32
k	1.99×10^{-6}	2.18×10^{-8}	4.66×10^{-6}	1.79×10^{-8}	9.76×10^{-7}	1.67×10^{-8}

from a tertiary carbon atom was found to be the most favorable CTP mechanism in alkyl acrylates. This study indicated that the monoradical $M_2^{\bullet}$ is as reactive as $M_1^{\bullet}$ in CTP reactions of methyl acrylate. Four different basis sets (6-31G(d), 6-31G(d,p), 6-311G(d), and 6-311G(d,p)) were applied to validate the calculated transition states and energy barriers. These basis sets predicted similar transition state geometries for the CTP mechanisms, activation energies with at most 10 kJ/mol difference, and rate constants with at most 2 orders of magnitude difference. The end substituent groups of the monomers were found to have little effect on the energy barriers of the CTP reactions. The study indicated that tertiary hydrogens of dead polymers formed by disproportionation reactions are most likely to be transferred to live polymer chains in CTP reactions. The levels of theory applied in this study are accurate enough to predict the mechanistic pathways and transition state structures, but further investigation with higher levels of theory is recommended. While the application of IEF-PCM showed strong solvent effects on the

DOI: 10.1021/ie504110n
Ind. Eng. Chem. Res. 2015, 54, 4148−4165

kinetic parameters of the CTP reactions of MA, EA, and *n*-BA in *n*-butanol, the application of COSMO showed no such remarkable effects.

■ ASSOCIATED CONTENT

Supporting Information

The transition state structure for the MA1-D1-1 mechanism (hydrogen atom abstraction from a tertiary carbon atom of a dead polymer chain initiated by $M_1^\bullet$) is shown in Figure 1. The energy differences of the optimized reactants and products for all possible mechanisms of chain transfer to the D1 dead polymer for MA, EA and *n*-BA are given in Tables 1, 2, and 3. Figure 2 presents the geometries of the transition state structures for the most probable CTP mechanisms involving a three [MA2-D1-1(a)] or four [MA2-D1-1(b)] MA-unit and a three EA-unit live chain initiated by $M_2^\bullet$. This material is available free of charge via the Internet at http://pubs.acs.org.

■ AUTHOR INFORMATION

Corresponding Author

*Tel.: (215) 895-1710; E-mail: ms1@drexel.edu.

Notes

The authors declare no competing financial interest.

■ ACKNOWLEDGMENTS

This material is based upon work partially supported by the National Science Foundation under Grants No. CBET-1160169 and CBET-1159736. Any opinions, findings, and conclusions or recommendations expressed in this material are those of the authors and do not necessarily reflect the views of the National Science Foundation. Acknowledgment is also made to the Donors of the American Chemical Society Petroleum Research Fund for partial support of this research. A.M.R. acknowledges the Department of Energy Office of Basic Energy Sciences Grant DE-FG02-07ER15920. S.L. acknowledges the National Science Foundation Grant No. CBET-1159736. Computational support was provided by the High-Performance Computing Modernization Office of the U.S. Department of Defense.

■ REFERENCES

(1) Song, J.; Thurber, C. M.; Kobayashi, S.; Baker, A. M.; Macosko, C. W.; Silvis, H. C. Blends of polyolefin/PMMA for improved scratch resistance, adhesion and compatibility. *Polymer* **2012**, *53* (16), 3636–3641.

(2) VOC's Directive, EU committee of the American chamber of commerce in Belgium, ASBL/VZw, Brussels, July 8, 1996, http://eur-lex.europa.eu/LexUriServ/LexUriServ.do?uri=CELEX:31996L0061:en:HTML.

(3) Campbell, J. D.; Teymour, F.; Morbidelli, M. High temperature free radical polymerization. 1. Investigation of continuous styrene polymerization. *Macromolecules* **2003**, *36* (15), 5491–5501.

(4) Wang, W.; Hutchinson, R. A. Recent advances in the study of high-temperature free radical acrylic solution copolymerization. *Macromol. React. Eng.* **2008**, *2* (3), 199–214.

(5) Hamielec, A. E.; Lawless, G. P.; Schultz, H. H. Process for continuous bulk copolymerization of vinyl monomers. US Patent 4 414 370, 1983.

(6) Cunningham, M. F.; Hutchinson, R. A. Industrial applications and processes. In *Handbook of Radical Polymerization*; Matyjaszewski, K., Davis, T. P., Eds.; John Wiley & Sons, Inc.: Hoboken, NJ, 2003; DOI: 10.1002/0471220450.ch7.

(7) Nikitin, A. N.; Hutchinson, R. A.; Wang, W.; Kalfas, G. A.; Richards, J. R.; Bruni, C. Effect of intramolecular transfer to polymer on stationary free-radical polymerization of alkyl acrylates, 5—Consideration of solution polymerization up to high temperatures. *Macromol. React. Eng.* **2010**, *4* (11–12), 691–706.

(8) Srinivasan, S.; Lee, M. W.; Grady, M. C.; Soroush, M.; Rappe, A. M. Computational study of the self-initiation mechanism in thermal polymerization of methyl acrylate. *J. Phys. Chem. A* **2009**, *113* (40), 10787–10794.

(9) Srinivasan, S.; Lee, M. W.; Grady, M. C.; Soroush, M.; Rappe, A. M. Self-initiation mechanism in spontaneous thermal polymerization of ethyl and *n*-butyl acrylate: A theoretical study. *J. Phys. Chem. A* **2010**, *114* (30), 7975–7983.

(10) Srinivasan, S.; Lee, M. W.; Grady, M. C.; Soroush, M.; Rappe, A. M. Computational evidence for self-initiation in spontaneous high-temperature polymerization of methyl methacrylate. *J. Phys. Chem. A* **2011**, *115* (6), 1125–1132.

(11) Yu, X. R.; Broadbelt, L. J. Kinetic study of 1,5-hydrogen transfer reactions of methyl acrylate and butyl acrylate using quantum chemistry. *Macromol. Theory Simul.* **2012**, *21* (7), 461–469.

(12) Nikitin, A. N.; Hutchinson, R. A.; Kalfas, G. A.; Richards, J. R.; Bruni, C. The effect of intramolecular transfer to polymer on stationary free-radical polymerization of alkyl acrylates, 3—Consideration of solution polymerization up to high conversions. *Macromol. Theory Simul.* **2009**, *18* (4–5), 247–258.

(13) Agirre, A.; Santos, J. I.; Etxeberria, A.; Sauerland, V.; Leiza, J. R. Polymerization of *n*-butyl acrylate with high concentration of a chain transfer agent (CBr4): Detailed characterization and impact on branching. *Polym. Chem.* **2013**, *4* (6), 2062–2079.

(14) Vandenbergh, J.; Junkers, T. Synthesis of macromonomers from high-temperature activation of nitroxide mediated polymerization (NMP)-made polyacrylates. *Macromolecules* **2013**, *46* (9), 3324–3331.

(15) Peck, A. N. F.; Hutchinson, R. A. Secondary reactions in the high-temperature free radical polymerization of butyl acrylate. *Macromolecules* **2004**, *37* (16), 5944–5951.

(16) Hamzehlou, S.; Reyes, Y.; Leiza, J. R. Detailed microstructure investigation of acrylate/methacrylate functional copolymers by kinetic monte carlo simulation. *Macromol. React. Eng.* **2012**, *6* (8), 319–329.

(17) Mavroudakis, E.; Cuccato, D.; Moscatelli, D. Theoretical study of chain transfer to agent kinetics in butyl acrylate polymerization. *Ind. Eng. Chem. Res.* **2014**, *53* (22), 9058–9066.

(18) Plessis, C.; Arzamendi, G.; Alberdi, J. M.; Agnely, M.; Leiza, J. R.; Asua, J. M. Intramolecular chain transfer to polymer in the emulsion polymerization of 2-ethylhexyl acrylate. *Macromolecules* **2001**, *34* (17), 6138–6143.

(19) Ahmad, N. M.; Heatley, F.; Lovell, P. A. Chain transfer to polymer in free-radical solution polymerization of *n*-butyl acrylate studied by NMR spectroscopy. *Macromolecules* **1998**, *31* (9), 2822–2827.

(20) Cuccato, D.; Mavroudakis, E.; Dossi, M.; Moscatelli, D. A density functional theory study of secondary reactions in *n*-butyl acrylate free radical polymerization. *Macromol. Theory Simul.* **2013**, *22* (2), 127–135.

(21) Cuccato, D.; Mavroudakis, E.; Moscatelli, D. Quantum chemistry investigation of secondary reaction kinetics in acrylate-based copolymers. *J. Phys. Chem. A* **2013**, *117* (21), 4358–4366.

(22) Chiefari, J.; Jeffery, J.; Mayadunne, R. T. A.; Moad, G.; Rizzardo, E.; Thang, S. H. Chain transfer to polymer: A convenient route to macromonomers. *Macromolecules* **1999**, *32* (22), 7700–7702.

(23) Reyes, Y.; Asua, J. M. Revisiting chain transfer to polymer and branching in controlled radical polymerization of butyl acrylate. *Macromol. Rapid Commun.* **2011**, *32* (1), 63–67.

(24) Rawlston, J. A.; Schork, F. J.; Grover, M. A. Multiscale modeling of branch length in butyl acrylate solution polymerization: Molecular versus continuum kinetics. *Macromol. Theory Simul.* **2011**, *20* (8), 645–659.

(25) Quan, C. L.; Soroush, M.; Grady, M. C.; Hansen, J. E.; Simonsick, W. J. High-temperature homopolymerization of ethyl acrylate and *n*-butyl acrylate: Polymer characterization. *Macromolecules* **2005**, *38* (18), 7619–7628.

DOI: 10.1021/ie504110n
Ind. Eng. Chem. Res. 2015, 54, 4148–4165

(26) Yu-Su, S. Y.; Sun, F. C.; Sheiko, S. S.; Konkolewicz, D.; Lee, H. I.; Matyjaszewski, K. Molecular imaging and analysis of branching topology in polyacrylates by atomic force microscopy. *Macromolecules* **2011**, *44* (15), 5928−5936.
(27) Liang, K.; Hutchinson, R. A. The effect of hydrogen bonding on intramolecular chain transfer in polymerization of acrylates. *Macromol. Rapid Commun.* **2011**, *32* (14), 1090−1095.
(28) Ahmad, N. M.; et al. Chain transfer to polymer and branching in controlled radical polymerizations of *n*-butyl acrylate. *Macromol. Rapid Commun.* **2009**, *30* (23), 2002−2021.
(29) Barth, J.; Buback, M.; Barner-Kowollik, C.; Junkers, T.; Russell, G. T. Single-pulse pulsed laser polymerization-electron paramagnetic resonance investigations into the termination kinetics of *n*-butyl acrylate macromonomers. *J. Polym. Sci., Part A: Polym. Chem.* **2012**, *50* (22), 4740−4748.
(30) Gilbert, B. C.; Smith, J. R. L.; Milne, E. C.; Whitwood, A. C.; Taylor, P. Kinetic and structural EPR studies of radical polymerization—monomer, dimer, trimer and midchain radicals formed via the initiation of polymerization of acrylic-acid and related-compounds with electrophilic radicals (·OH,SO_4 radical-ion and Cl_2 radical-ion). *J. Chem. Soc., Perkin Trans. 2* **1994**, No. 8, 1759−1769.
(31) Yamada, B.; Azukizawa, M.; Yamazoe, H.; Hill, D. J. T.; Pomery, P. J. Free radical polymerization of cyclohexyl acrylate involving interconversion between propagating and mid-chain radicals. *Polymer* **2000**, *41* (15), 5611−5618.
(32) Azukizawa, M.; Yamada, B.; Hill, D. J. T.; Pomery, P. J. Radical polymerization of phenyl acrylate as studied by ESR spectroscopy: Concurrence of propagating and mid-chain radicals. *Macromol. Chem. Phys.* **2000**, *201* (7), 774−781.
(33) Plessis, C.; Arzamendi, G.; Leiza, J. R.; Schoonbrood, H. A. S.; Charmot, D.; Asua, J. M. A decrease in effective acrylate propagation rate constants caused by intramolecular chain transfer. *Macromolecules* **2000**, *33* (1), 4−7.
(34) Farcet, C.; Belleney, J.; Charleux, B.; Pirri, R. Structural characterization of nitroxide-terminated poly(*n*-butyl acrylate) prepared in bulk and miniemulsion polymerizations. *Macromolecules* **2002**, *35* (13), 4912−4918.
(35) Plessis, C.; Arzamendi, G.; Alberdi, J. M.; van Herk, A. M.; Leiza, J. R.; Asua, J. M. Evidence of branching in poly(butyl acrylate) produced in pulsed-laser polymerization experiments. *Macromol. Rapid Commun.* **2003**, *24* (2), 173−177.
(36) Santanakrishnan, S.; Tang, L.; Hutchinson, R. A.; Stach, M.; Lacik, I.; Schrooten, J.; Hesse, P.; Buback, M. Kinetics and modeling of batch and semibatch aqueous-phase NVP free-radical polymerization. *Macromol. React. Eng.* **2010**, *4* (8), 499−509.
(37) Plessis, C.; Arzamendi, G.; Leiza, J. R.; Schoonbrood, H. A. S.; Charmot, D.; Asua, J. M. Modeling of seeded semibatch emulsion polymerization of *n*-BA. *Ind. Eng. Chem. Res.* **2001**, *40* (18), 3883−3894.
(38) Angoy, M.; Bartolome, M. I.; Vispe, E.; Lebeda, P.; Jimenez, M. V.; Perez-Torrente, J. J.; Collins, S.; Podzimek, S. Branched poly(phenylacetylene). *Macromolecules* **2010**, *43* (15), 6278−6283.
(39) Tobing, S. D.; Klein, A. Molecular parameters and their relation to the adhesive performance of acrylic pressure-sensitive adhesives. *J. Appl. Polym. Sci.* **2001**, *79* (12), 2230−2244.
(40) Ahmad, N. M.; Britton, D.; Heatley, F.; Lovell, P. A. Chain transfer to polymer in emulsion polymerization. *Macromol. Symp.* **1999**, *143*, 231−241.
(41) Lovell, P. A.; Shah, T. H.; Heatley, F. Chain transfer to polymer in emulsion polymerization of *n*-butyl acrylate studied by carbon-13 NMR spectroscopy and gel permeation chromatography. *Polym. Commun.* **1991**, *32*, 98−103.
(42) Arzamendi, G.; Plessis, C.; Leiza, J. R.; Asua, J. M. Effect of the intramolecular chain transfer to polymer on PLP/SEC experiments of alkyl acrylates. *Macromol. Theory Simul.* **2003**, *12* (5), 315−324.
(43) Nikitin, A. N.; Castignolles, P.; Charleux, B.; Vairon, J. P. Simulation of molecular weight distributions obtained by pulsed laser polymerization (PLP): New analytical expressions including intramolecular chain transfer to the polymer. *Macromol. Theory Simul.* **2003**, *12* (6), 440−448.
(44) Nikitin, A. N.; Castignolles, P.; Charleux, B.; Vairon, J. P. Determination of propagation rate coefficient of acrylates by pulsed-laser polymerization in the presence of intramolecular chain transfer to polymer. *Macromol. Rapid Commun.* **2003**, *24* (13), 778−782.
(45) Nikitin, A. N.; Hutchinson, R. A. The effect of intramolecular transfer to polymer on stationary free radical polymerization of alkyl acrylates. *Macromolecules* **2005**, *38* (5), 1581−1590.
(46) Nikitin, A. N.; Hutchinson, R. A. Effect of intramolecular transfer to polymer on stationary free radical polymerization of alkyl acrylates, 2—Improved consideration of termination. *Macromol. Theory Simul.* **2006**, *15* (2), 128−136.
(47) Irzhak, T. F.; Irzhak, V. I. Kinetics of formation of the topological structure during radical polymerization accompanied by the reaction of chain transfer to the polymer. *Polym. Sci. Ser. B* **2013**, *55* (5−6), 391−399.
(48) Mavroudakis, E.; Cuccato, D.; Moscatelli, D. Quantum mechanical investigation on bimolecular hydrogen abstractions in butyl acrylate-based free radical polymerization processes. *J. Phys. Chem. A* **2014**, *118*, 1799−1806.
(49) Heatley, F.; Lovell, P. A.; Yamashita, T. Chain transfer to polymer in free-radical solution polymerization of 2-ethylhexyl acrylate studied by NMR spectroscopy. *Macromolecules* **2001**, *34* (22), 7636−7641.
(50) Adamsons, K.; Blackman, G.; Gregorovich, B.; Lin, L.; Matheson, R. Oligomers in the evolution of automotive clearcoats: mechanical performance testing as a function of exposure. *Prog. Org. Coat.* **1998**, *34* (1−4), 64−74.
(51) Haseebuddin, S.; Raju, K.; Yaseen, M. Applicability of the WLF equation to polyurethane polyols and film properties of their resins. *Prog. Org. Coat.* **1997**, *30* (1−2), 25−30.
(52) Grady, M. C.; Simonsick, W. J.; Hutchinson, R. A. Studies of higher temperature polymerization of *n*-butyl methacrylate and *n*-butyl acrylate. *Macromol. Symp.* **2002**, *182*, 149−168.
(53) Nikitin, A. N.; Hutchinson, R. A.; Buback, M.; Hesse, P. Determination of intramolecular chain transfer and midchain radical propagation rate coefficients for butyl acrylate by pulsed laser polymerization. *Macromolecules* **2007**, *40* (24), 8631−8641.
(54) Buback, M.; Gilbert, R. G.; Hutchinson, R. A.; Klumperman, B.; Kuchta, F. D.; Manders, B. G.; Odriscoll, K. F.; Russell, G. T.; Schweer, J. Critically evaluated rate coefficients for free-radical polymerization. 1. Propagation rate coefficient for styrene. *Macromol. Chem. Phys.* **1995**, *196* (10), 3267−3280.
(55) Beuermann, S.; Buback, M.; Davis, T. P.; Gilbert, R. G.; Hutchinson, R. A.; Olaj, O. F.; Russell, G. T.; Schweer, J.; vanHerk, A. M. Critically evaluated rate coefficients for free-radical polymerization. 2. Propagation rate coefficients for methyl methacrylate. *Macromol. Chem. Phys.* **1997**, *198* (5), 1545−1560.
(56) Nikitin, A. N.; Hutchinson, R. A.; Buback, M.; Hesse, P. A novel approach for investigation of chain transfer events by pulsed laser polymerization. *Macromol. Chem. Phys.* **2011**, *212* (7), 699−707.
(57) Asua, J. M.; Beuermann, S.; Buback, M.; Castignolles, P.; Charleux, B.; Gilbert, R. G.; Hutchinson, R. A.; Leiza, J. R.; Nikitin, A. N. Critically evaluated rate coefficients for free-radical polymerization, 5—Propagation rate coefficient for butyl acrylate. *Macromol. Chem. Phys.* **2004**, *205* (16), 2151−2160.
(58) Barner-Kowollik, C.; Gunzler, F.; Junkers, T. Pushing the limit: Pulsed laser polymerization of *n*-butyl acrylate at 500 Hz. *Macromolecules* **2008**, *41* (23), 8971−8973.
(59) Rantow, F. S.; Soroush, M.; Grady, M. C.; Kalfas, G. A. Spontaneous polymerization and chain microstructure evolution in high-temperature solution polymerization of *n*-butyl acrylate. *Polymer* **2006**, *47* (4), 1423−1435.
(60) Wang, W.; Nikitin, A. N.; Hutchinson, R. A. Consideration of macromonomer reactions in *n*-butyl acrylate free radical polymerization. *Macromol. Rapid Commun.* **2009**, *30* (23), 2022−2027.
(61) Buback, M.; Kling, M.; Schmatz, S. Decomposition of tertiary alkoxy radicals. *Z. Phys. Chem.* **2005**, *219* (9), 1205−1222.

DOI: 10.1021/ie504110n
Ind. Eng. Chem. Res. 2015, 54, 4148−4165

(62) Wong, M. W.; Radom, L. Radical-addition to alkenes—An assessment of theoretical procedures. *J. Phys. Chem.* **1995**, *99* (21), 8582−8588.
(63) Scott, A. P.; Radom, L. Harmonic vibrational frequencies: An evaluation of Hartree-Fock, Möller-Plesset, quadratic configuration interaction, density functional theory, and semiempirical scale factors. *J. Phys. Chem.* **1996**, *100* (41), 16502−16513.
(64) Heuts, J. P. A.; Gilbert, R. G.; Radom, L. Determination of arrhenius parameters for propagation in free-radical polymerizations: An assessment of ab initio procedures. *J. Phys. Chem.* **1996**, *100* (49), 18997−19006.
(65) Huang, D. M.; Monteiro, M. J.; Gilbert, R. G. A theoretical study of propagation rate coefficients for methacrylonitrile and acrylonitrile. *Macromolecules* **1998**, *31* (16), 5175−5187.
(66) Van Speybroeck, V.; Van Cauter, K.; Coussens, B.; Waroquier, M. Ab initio study of free-radical polymerizations: Cost-effective methods to determine the reaction rates. *ChemPhysChem* **2005**, *6* (1), 180−189.
(67) Heuts, J. P. A.; Gilbert, R. G.; Radom, L. A priori prediction of propagation rate coefficients in free-radical polymerizations: Propagation of ethylene. *Macromolecules* **1995**, *28* (26), 8771−8781.
(68) Khuong, K. S.; Jones, W. H.; Pryor, W. A.; Houk, K. N. The mechanism of the self-initiated thermal polymerization of styrene. Theoretical solution of a classic problem. *J. Am. Chem. Soc.* **2005**, *127* (4), 1265−1277.
(69) Gunaydin, H.; Salman, S.; Tuzun, N. S.; Avci, D.; Aviyente, V. Modeling the free radical polymerization of acrylates. *Int. J. Quantum Chem.* **2005**, *103* (2), 176−189.
(70) Arnaud, R.; Vetere, V.; Barone, V. Quantum mechanical study of regioselectivity of radical additions to substituted olefins. *J. Comput. Chem.* **2000**, *21* (8), 675−691.
(71) Van Cauter, K.; Van Speybroeck, V.; Vansteenkiste, P.; Reyniers, M. F.; Waroquier, M. Ab initio study of free-radical polymerization: Polyethylene propagation kinetics. *ChemPhysChem* **2006**, *7* (1), 131−140.
(72) Hohenberg, P.; Kohn, W. Imhomogenous electron gas. *Phys. Rev.* **1964**, *136*, 864.
(73) Rodriguez-Sanchez, I.; Armando Zaragoza-Contreras, E.; Glossman-Mitnik, D. Theoretical evaluation of the order of reactivity of transfer agents utilized in RAFT polymerization. *J. Mol. Model.* **2010**, *16* (1), 95−105.
(74) Lin, C. Y.; Coote, M. L.; Petit, A.; Richard, P.; Poli, R.; Matyjaszewski, K. Ab initio study of the penultimate effect for the ATRP activation step using propylene, methyl acrylate, and methyl methacrylate monomers. *Macromolecules* **2007**, *40* (16), 5985−5994.
(75) Izgorodina, E. I.; Coote, M. L. Reliable low-cost theoretical procedures for studying addition-fragmentation in RAFT polymerization. *J. Phys. Chem. A* **2006**, *110* (7), 2486−2492.
(76) Liu, S.; Srinivasan, S.; Tao, J. M.; Grady, M. C.; Soroush, M.; Rappe, A. M. Modeling spin-forbidden monomer self-initiation reactions in spontaneous free-radical polymerization of acrylates and methacrylates. *J. Phys. Chem. A* **2014**, *118* (40), 9310−9318.
(77) Coote, M. L. The kinetics of addition and fragmentation in reversible addition fragmentation chain transfer polymerization: An ab initio study. *J. Phys. Chem. A* **2005**, *109* (6), 1230−1239.
(78) Parr, R. G.; Yang, W. In *Density-Functional Theory of Atoms and Molecules*; Oxford University Press: New York, 1989.
(79) Dreizler, R. M.; Gross, E. K. U. In *Density-Functional Theory: An Approach to the Quantum Many-Body Problem*; Springer-Verlag: Berlin, Heidelberg, 1990
(80) Liu, S.; Srinivasan, S.; Grady, M. C.; Soroush, M.; Rappe, A. M. Computational study of cyclohexanone-monomer co-initiation mechanism in thermal homo-polymerization of methyl acrylate and methyl methacrylate. *J. Phys. Chem. A* **2012**, *116* (22), 5337−5348.
(81) Yu, X.; Pfaendtner, J.; Broadbelt, L. J. Ab initio study of acrylate polymerization reactions: Methyl methacrylate and methyl acrylate propagation. *J. Phys. Chem. A* **2008**, *112* (29), 6772−6782.
(82) Moghadam, N.; Liu, S.; Srinivasan, S.; Grady, M. C.; Soroush, M.; Rappe, A. M. Computational study of chain transfer to monomer reactions in high-temperature polymerization of alkyl acrylates. *J. Phys. Chem. A* **2013**, *117* (12), 2605−2618.
(83) Moghadam, N.; Srinivasan, S.; Grady, M. C.; Rappe, A. M.; Soroush, M. Theoretical study of chain transfer to solvent reactions of alkyl acrylates. *J. Phys. Chem. A* **2014**, *118* (29), 5474−5487.
(84) Srinivasan, S.; Kalfas, G.; Petkovska, V. I.; Bruni, C.; Grady, M. C.; Soroush, M. Experimental study of the spontaneous thermal homopolymerization of methyl and *n*-butyl acrylate. *J. Appl. Polym. Sci.* **2010**, *118* (4), 1898−1909.
(85) Gora, R. W.; Bartkowiak, W.; Roszak, S.; Leszczynski, J. Intermolecular interactions in solution: Elucidating the influence of the solvent. *J. Chem. Phys.* **2004**, *120* (6), 2802−2813.
(86) Szafran, M.; Karelson, M. M.; Katritzky, A. R.; Koput, J.; Zerner, M. C. Reconsideration of solvent effects calculated by semiempirical quantum chemical methods. *J. Comput. Chem.* **1993**, *14* (3), 371−377.
(87) Tomasi, J.; Mennucci, B.; Cammi, R. Quantum mechanical continuum solvation models. *Chem. Rev.* **2005**, *105* (8), 2999−3093.
(88) Cammi, R.; Mennucci, B.; Tomasi, J. On the calculation of local field factors for microscopic static hyperpolarizabilities of molecules in solution with the aid of quantum-mechanical methods. *J. Phys. Chem. A* **1998**, *102* (5), 870−875.
(89) Thickett, S. C.; Gilbert, R. G. Propagation rate coefficient of acrylic acid: Theoretical investigation of the solvent effect. *Polymer* **2004**, *45* (20), 6993−6999.
(90) Klamt, A.; Schuurmann, G. COSMO—A new approach to dielectric screening in solvents with explicit expressions for the screening energy and its gradient. *J. Chem. Soc., Perkin Trans. 2* **1993**, No. 5, 799−805.
(91) Izgorodina, E. I.; Coote, M. L. Accurate ab initio prediction of propagation rate coefficients in free-radical polymerization: Acrylonitrile and vinyl chloride. *Chem. Phys.* **2006**, *324* (1), 96−110.
(92) Fu, K. X.; Zhu, Q.; Li, X. Y.; Gong, Z.; Ma, J. Y.; He, R. X. Continuous medium theory for nonequilibrium solvation: IV. Solvent reorganization energy of electron transfer based on conductor-like screening model. *J. Comput. Chem.* **2006**, *27* (3), 368−374.
(93) Mennucci, B.; Cances, E.; Tomasi, J. Evaluation of solvent effects in isotropic and anisotropic dielectrics and in ionic solutions with a unified integral equation method: Theoretical bases, computational implementation, and numerical applications. *J. Phys. Chem. B* **1997**, *101* (49), 10506−10517.
(94) Cances, E.; Mennucci, B.; Tomasi, J. A new integral equation formalism for the polarizable continuum model: Theoretical background and applications to isotropic and anisotropic dielectrics. *J. Chem. Phys.* **1997**, *107* (8), 3032−3041.
(95) Furuncuoglu, T.; Ugur, I.; Degirmenci, I.; Aviyente, V. Role of chain transfer agents in free radical polymerization kinetics. *Macromolecules* **2010**, *43* (4), 1823−1835.
(96) Watson, L. A.; Eisenstein, O. Entropy explained: The origin of some simple trends. *J. Chem. Educ.* **2002**, *79*, 1269−1277.
(97) Page, M. I. The energetics of neighbouring group participation. *Chem. Soc. Rev.* **1973**, *2*, 295−323.
(98) Yu, X.; Levine, S. E.; Broadbelt, L. J. Kinetic study of the copolymerization of methyl methacrylate and methyl acrylate using quantum chemistry. *Macromolecules* **2008**, *41*, 8242−8251.
(99) Page, M. I.; Jencks, W. P. Entropic contributions to rate accelerations in enzymic and intramolecular reactions and the chelate effect. *Proc. Nat. Acad. Sci. U.S.A.* **1971**, *68*, 1678−1683.
(100) Zhao, Y.; Truhlar, D. G. The M06 suite of density functionals for main group thermochemistry, thermochemical kinetics, noncovalent interactions, excited states, and transition elements: Two new functionals and systematic testing of four M06-class functionals and 12 other functionals. *Theor. Chem. Acc.* **2008**, *120* (1−3), 215−241.
(101) Zhao, Y.; Truhlar, D. G. Density functionals with broad applicability in chemistry. *Acc. Chem. Res.* **2008**, *41* (2), 157−167.
(102) Zhao, Y.; Truhlar, D. G. How well can new-generation density functionals describe the energetics of bond-dissociation reactions producing radicals? *J. Phys. Chem. A* **2008**, *112* (6), 1095−1099.
(103) Precomputed vibrational scaling factors. http://cccbdb.nist.gov/vibscalejust.asp (accessed February 2012).

DOI: 10.1021/ie504110n
Ind. Eng. Chem. Res. 2015, 54, 4148−4165

(104) Schmidt, M. W.; Baldridge, K. K.; Boatz, J. A.; Elbert, S. T.; Gordon, M. S.; Jensen, J. H.; Koseki, S.; Matsunaga, N.; Nguyen, K. A.; Su, S.; Windus, T. L.; Dupuis, M.; Montgomery, J. A., Jr. General atomic and molecular electronic-structure system. *J. Comput. Chem.* **1993**, *14* (11), 1347−1363 http://www.msg.ameslab.gov/GAMESS/GAMESS.html.
(105) Eyring, H. The activated complex in chemical reactions. *J. Chem. Phys.* **1935**, *3*, 107−115.
(106) McMahon, R. J. Chemical reactions involving quantum tunneling. *Science* **2003**, *299*, 833−834.
(107) Wigner, E. Calculation of the rate of elementary association reactions. *J. Chem. Phys.* **1937**, *5*, 720−725.
(108) Willemse, R. X. E.; van Herk, A. M.; Panchenko, E.; Junkers, T.; Buback, M. PLP-ESR monitoring of midchain radicals in *n*-butyl acrylate polymerization. *Macromolecules* **2005**, *38* (12), 5098−5103.
(109) Buback, M.; Hesse, P.; Junkers, T.; Sergeeva, T.; Theist, T. PLP labeling in ESR spectroscopic analysis of secondary and tertiary acrylate propagating radicals. *Macromolecules* **2008**, *41* (2), 288−291.
(110) Zhao, Y.; Schultz, N. E.; Truhlar, D. G. Design of density functionals by combining the method of constraint satisfaction with parametrization for thermochemistry, thermochemical kinetics, and noncovalent interactions. *J. Chem. Theory Comput.* **2006**, *2* (2), 364−382.
(111) Zhao, Y.; Schultz, N. E.; Truhlar, D. G. Exchange-correlation functional with broad accuracy for metallic and nonmetallic compounds, kinetics, and noncovalent interactions. *J. Chem. Phys.* **2005**, *123* (16).
(112) Liu, S.; Srinivasan, S.; Grady, M. C.; Soroush, M.; Rappe, A. M. Backbiting and beta-scission reactions in free-radical polymerization of methyl acrylate. *Int. J. Quantum Chem.* **2014**, *114* (5), 345−360.
(113) Sharp, K. Entropy-enthalpy compensation: Fact or artifact? *Protein Sci.* **2001**, *10* (3), 661−667.
(114) Van Leeuwen, R.; Baerends, E. J. Exchange-correlation potential with correct asymptotic behavior. *Phys. Rev. A* **1994**, *49*, 2421−2431.
(115) Becke, A. D. A new inhomogeneity parameter in DFT. *J. Chem. Phys.* **1998**, *109*, 2092−2098.
(116) Mori-Sanchez, P.; Cohen, A. J.; Yang, W. Many-electron self-interaction error in approximate density functionals. *J. Chem. Phys.* **2006**, *124*.
(117) Barth, J.; Buback, M.; Russell, G. T.; Smolne, S. Chain-length-dependent termination in radical polymerization of acrylates. *Macromol. Chem. Phys.* **2011**, *212* (13), 1366−1378.
(118) Liang, K.; Hutchinson, R. A.; Barth, J.; Samrock, S.; Buback, M. Reduced branching in poly(butyl acrylate) via solution radical polymerization in *n*-butanol. *Macromolecules* **2011**, *44*, 5843−5845.

DOI: 10.1021/ie504110n
Ind. Eng. Chem. Res. 2015, 54, 4148−4165